Journal of Paleontology, page 1 of 17

0022-3360/22/1937-2337
doi: 10.1017/jpa.2022.97

JOURNAL OF PALEONTOLOGY
A PUBLICATION OF THE Paleontological SOCIETY

The rangeomorph fossil *Charnia* from the Ediacaran Shibantan biota in the Yangtze Gorges area, South China

Chengxi Wu,[1,2] Ke Pang,[1,2]* Zhe Chen,[1,2]* Xiaopeng Wang,[1,2] Chuanming Zhou,[1,2] Bin Wan,[1,2] Xunlai Yuan,[1,2] and Shuhai Xiao[3]

[1]State Key Laboratory of Palaeobiology and Stratigraphy, Nanjing Institute of Geology and Palaeontology, and Center for Excellence in Life and Palaeoenvironment, Chinese Academy of Sciences, Nanjing 210008, China <cxwu@nigpas.ac.cn>, <kepang@nigpas.ac.cn>, <zhechen@nigpas.ac.cn>, <xpwang@nigpas.ac.cn>, <cmzhou@nigpas.ac.cn>, <binwan@nigpas.ac.cn>, <xlyuan@nigpas.ac.cn>
[2]University of Chinese Academy of Sciences, Beijing 100049, China
[3]Department of Geosciences, Virginia Tech, Blacksburg, VA 24061, USA <xiao@vt.edu>

Abstract.—The terminal Ediacaran Shibantan biota (~550–543 Ma) from the Dengying Formation in the Yangtze Gorges area of South China represents one of the rare examples of carbonate-hosted Ediacara-type macrofossil assemblages. In addition to the numerically dominant taxa—the non-biomineralizing tubular fossil *Wutubus* and discoidal fossils *Aspidella* and *Hiemalora*, the Shibantan biota also bears a moderate diversity of frondose fossils, including *Pteridinium*, *Rangea*, *Arborea*, and *Charnia*. In this paper, we report two species of the rangeomorph genus *Charnia*, including the type species *Charnia masoni* Ford, 1958 emend. and *Charnia gracilis* new species, from the Shibantan biota. Most of the Shibantan *Charnia* specimens preserve only the petalodium, with a few bearing the holdfast and stem. Despite overall architectural similarities to other *Charnia* species, the Shibantan specimens of *Charnia gracilis* n. sp. are distinct in their relatively straight, slender, and more acutely angled first-order branches. They also show evidence that may support a two-stage growth model and a epibenthic sessile lifestyle. *Charnia* fossils described herein represent one of the youngest occurrences of this genus and extend its paleogeographic and stratigraphic distributions. Our discovery also highlights the notable diversity of the Shibantan biota, which contains examples of a wide range of Ediacaran morphogroups.

UUID: http://zoobank.org/837216cd-4a4a-4e13-89e2-ee354ba48a4c

Introduction

The late Ediacaran Period witnessed the rise and fall of the Ediacaran macrobiota (~574–539 Ma; Linnemann et al., 2019; Matthews et al., 2021), a group of macro-organisms that are complex and soft-bodied. Although some of the Ediacara-type macro-organisms are very likely metazoans (Fedonkin and Waggoner, 1997; Bobrovskiy et al., 2018; Chen et al., 2019), most of them remain phylogenetically unresolved. The Ediacaran macrobiota consists of three assemblages that may broadly represent three stages of evolution (Waggoner, 2003), although environmental conditions may have also played a role in their spatio-temporal distribution (Gehling and Droser, 2013; Grazhdankin, 2014). These stages are exemplified by the Avalon (~574–560 Ma), White Sea (~560–550 Ma), and Nama (~550–539 Ma) assemblages (Waggoner, 2003; Boag et al., 2016). Overall, the three assemblages have distinct taxonomic groupings and representative taxa, although a small number of taxa, for example, the frondose fossil *Arborea*, are known to occur in all three assemblages (Xiao and Laflamme, 2009; Droser et al., 2017). Like *Arborea*, the rangeomorph fossil *Charnia* is also previously known from the Avalon (Hofmann et al., 2008; Narbonne et al., 2014; Liu et al., 2015; Wilby et al., 2015), White Sea (Martin et al., 2000; Gehling and Droser, 2013), and Nama assemblages (Grazhdankin et al., 2008), therefore representing one of the longest-ranging genera of Ediacara-type macrofossils in terms of stratigraphic distribution.

Charnia was first described from the Ediacaran Charnian Supergroup in England (Ford, 1958). It is perhaps one of the most studied taxa of the Ediacara-type macro-organisms (Laflamme et al., 2007; Antcliffe and Brasier, 2008; Dunn et al., 2018, 2019, 2021; Butterfield, 2022). Different phylogenetic affinities for *Charnia* have been proposed since its discovery. It was originally described as an alga (Ford, 1958) but later classified into the family Charniidae (Glaessner, 1979), which may belong to the class Rangeomorpha of a proposed extinct phylum, the Petalonamae (Pflug, 1970, 1972; Jenkins, 1985). *Charnia* and other rangeomorphs have been variously interpreted as pennatulacean cnidarians (Glaessner, 1959. 1984; Glaessner and Wade, 1966; Gehling, 1991), lichens (Retallack, 1994), fungi (Peterson et al., 2003), members of the extinct kingdom Vendobionta (Seilacher, 1992), or members within the total-group Metazoa (e.g., Xiao and Laflamme, 2009; Dunn et al., 2018; Butterfield, 2022). Although *Charnia* and modern sea pens both possess a similar leaf-like shape, ontogenetic analysis reveals that *Charnia* and modern sea pens may have opposite growth polarities (Antcliffe and Brasier, 2007, 2008).

*Corresponding author

Recently, detailed morphological descriptions and functional analyses, coupled with cladistic investigations (Dececchi et al., 2017, 2018), have led to the phylogenetic interpretations of rangeomorphs as stem-group metazoans (Xiao and Laflamme, 2009; Budd and Jensen, 2017; Darroch et al., 2018; Dunn et al., 2018), stem-group eumetazoans (Dunn et al., 2018, 2021; Hoyal Cuthill and Han, 2018; Butterfield, 2022; Runnegar, 2022), or stem-group cnidarians (Dunn et al., 2018; Butterfield, 2022). The feeding strategy of rangeomorphs also remains debated. Several studies have suggested that rangeomorphs, as well as erniettomorphs and dickinsoniomorphs, may have been capable of osmotrophy due to their high surface area to volume (SA/V) ratios (Laflamme et al., 2009; Sperling and Vinther, 2010; Ghisalberti et al., 2014). Liu et al. (2015) argued that osmotrophy in rangeomorphs may have been limited by the availability and recalcitrant nature of dissolved organic carbon. In addition, Butterfield (2022) contended that the large size, hence elevated Reynolds and Péclet numbers, of rangeomorphs are not conducive for osmotrophy. Alternative feeding strategies of rangeomorphs include suspension feeding (Butterfield, 2022) and intracellular symbiosis (Dufour and McIlroy, 2016; McIlroy et al., 2021), but these hypotheses have not been critically evaluated on the basis of detailed morphological observation and theoretical modeling.

The occurrence of *Charnia* in the Shibantan biota was first reported by S. Xiao et al. (2020), but a detailed description and morphometric assessment were not presented. Here we provide a systematic description of *Charnia* fossils, including the type species *C. masoni* Ford, 1958 emend. and *C. gracilis* n. sp., from this Lagerstätte. The fossils are preserved in thin-bedded bituminous limestone, which was deposited in subtidal environment (Q. Xiao et al., 2020), from the terminal Ediacaran Shibantan Member of the Dengying Formation in the Yangtze Gorges area of South China. The Shibantan Member is geochronologically constrained to between ~550 Ma and ~543 Ma (Huang et al., 2020; Yang et al., 2021). Thus, these Shibantan specimens not only extend the paleogeographic and paleoenvironmental distributions of *Charnia*, but also represent one of the youngest fossil records of this genus. They help us to obtain a more comprehensive picture of the rise and fall of the Ediacara-type macro-organisms.

Materials and methods

The Ediacaran succession in the Yangtze Gorges area of South China consists of the Doushantuo and Dengying formations (Fig. 1.1). The Dengying Formation consists of three lithostratigraphic members: the Hamajing, Shibantan, and Baimatuo members, in ascending order (Fig. 1.2). It is constrained by two CA-ID-TIMS zircon U–Pb ages of 551.1 ± 0.7 Ma (Condon et al., 2005) and 550.1 ± 0.6 Ma (Yang et al., 2021) from the uppermost Miaohe Member, which is regarded as the uppermost Doushantuo Formation (Xiao et al., 2017; Zhou et al., 2017; but see An et al., 2015), and a SIMS zircon U–Pb age of 543.4 ± 3.5 Ma from the Baimatuo Member (Huang et al., 2020).

The Hamajing and Baimatuo members are both characterized by dolostones with peritidal structures, such as tepees, karstification structures, and dissolution vugs (Duda et al., 2016; Y. Ding et al., 2019; S. Xiao et al., 2020). The Shibantan Member consists of 100–150 m dark gray, medium- to thin-bedded bituminous limestone with diagenetic chert nodules and bands (Chen et al., 2014; S. Xiao et al., 2020). Fine and crinkled laminae are dominant in the Shibantan Member, but hummocky cross-beds, rip-up clasts, intraclastic breccias, and graded beds are also common. Indeed, intraclastic breccias and graded beds in the Shibantan Member are interpreted as tempestites that were laid down in a subtidal environment between fair-weather and storm-wave bases (Q. Xiao et al., 2020). These tempestites may have contributed to the rapid burial of the soft-bodied Ediacara-type macrofossils (Q. Xiao et al., 2020). The wrinkled surfaces and dark crinkled micro-laminae in the Shibantan Member, interpreted as evidence for microbial mats (Chen et al., 2013; Meyer et al., 2014), may have played an important role in the preservation of the soft-bodied Ediacara-type macrofossils (Gehling, 1999; Callow and Brasier, 2009; Laflamme et al., 2011). These microbial mats, probably constructed mainly by cyanobacteria, have close associations with trace fossils from the Shibantan Member and may suggest that they provided oxygen oases as well as nutrients for the trace makers (Chen et al., 2013; Meyer et al., 2014; W. Ding et al., 2019; Xiao et al., 2019).

The *Charnia* fossils described here were collected from the Shibantan limestone at the Wuhe quarry (30.789°N, 111.051°E; Fig. 1.1), where a number of diverse fossils are preserved (S. Xiao et al., 2020). The Shibantan biota consists of algal fossils, Ediacara-type macrofossils, trace fossils, and some problematic fossils (S. Xiao et al., 2020). Recently, biomineralizing tubular fossils have also been discovered in the Baimatuo Member (Liang et al., 2020; Zhang et al., 2022) and also likely in the upper Shibantan Member (Chen et al., 2016), but these tubular fossils may be younger than the soft-bodied Ediacara-type macrofossils from Wuhe quarry. There are several frondose genera among the Ediacara-type macrofossils of the Shibantan biota (S. Xiao et al., 2020), including *Arborea*, *Rangea*, *Pteridinium* (Chen et al., 2014; Wang et al., 2020), and *Charnia* (herein). The *Charnia* specimens were collected from the basal Shibantan Member (Fig. 1.2) with known stratigraphic orientation (to determine whether fossils are preserved on the top or bottom bedding surface). Specimens were photographed with a Nikon D810 digital camera, and measurements of the specimens were carried out on these photos using ImageJ software. Specimens from Charnwood Forest in the United Kingdom (Wilby et al., 2015; Dunn et al., 2018, 2019, 2021), Newfoundland in Canada (Laflamme et al., 2007; Hofmann et al., 2008; Liu et al., 2013, 2015; Dunn et al., 2019), Sekwi Brook in Northwest Canada (Narbonne et al., 2014), the White Sea region and Olenek Uplift, Siberia in Russia (Sokolov and Fedonkin, 1984; Runnegar and Fedonkin, 1992; Grazhdankin and Bronnikov, 1997; Martin et al., 2000; Grazhdankin et al., 2008), Flinders Ranges, South Australia (Glaessner and Wade, 1966; Nedin and Jenkins, 1998; Gehling and Droser, 2013), and Oulongbuluke terrane in Northwest China (Pang et al., 2021) were also measured for comparison (Table 1). Measurements on Newfoundland specimens were conducted on retrodeformed photos from cited sources to account for tectonic deformation of the sediments.

Repository and institutional abbreviation.—Specimens of *Charnia* illustrated in this study are reposited in Nanjing

https://doi.org/10.1017/jpa.2022.97 Published online by Cambridge University Press

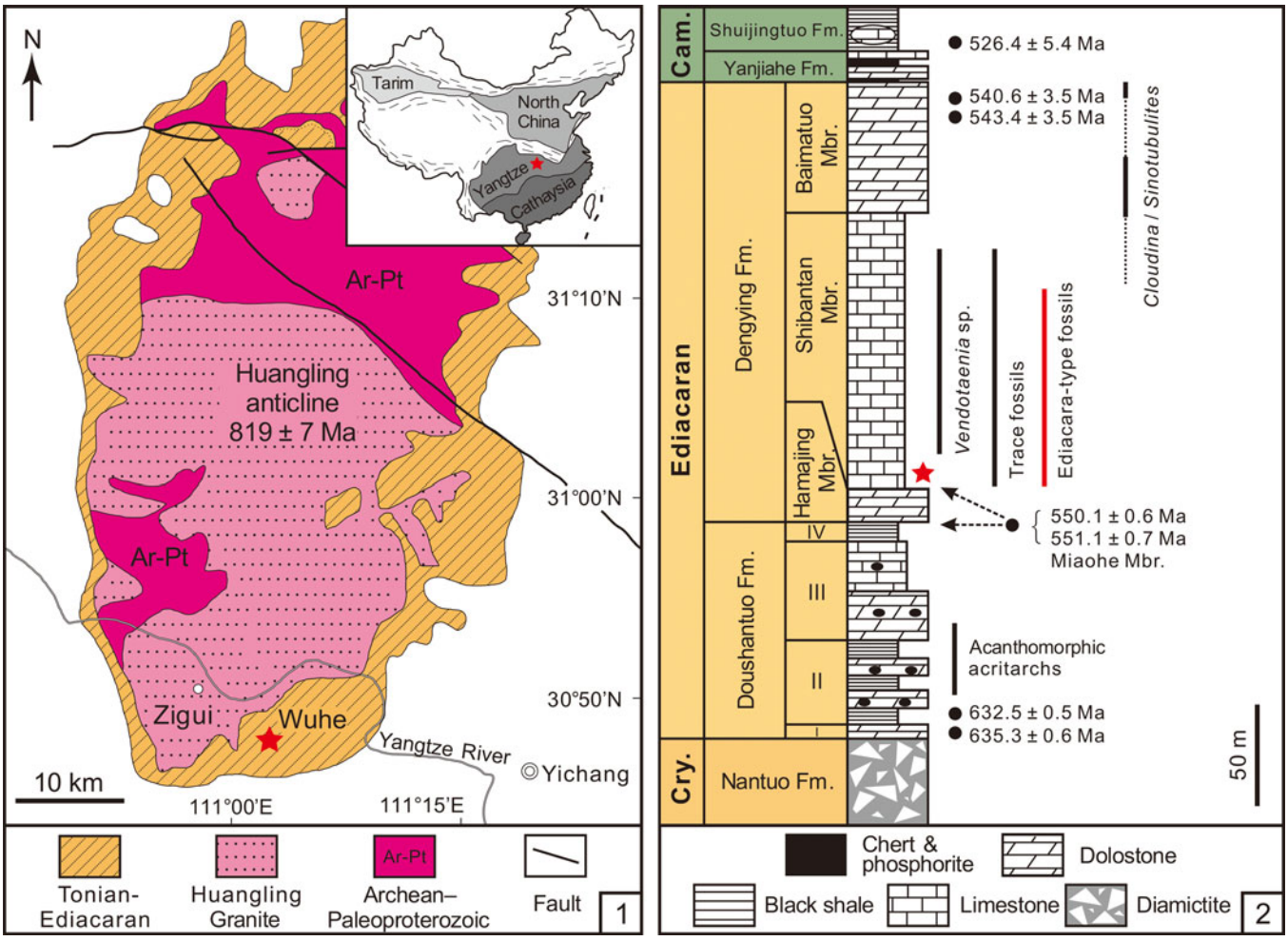

Figure 1. (**1**) Geological map of the Wuhe section in the Yangtze Gorges area with location of the Wuhe quarry (marked with a red star) and the Huangling anticline in the Yangtze Gorges area. Inset map shows the location of the Huangling anticline (red star) and major tectonic terranes in China. (**2**) Generalized stratigraphic column of the Ediacaran succession in the Yangtze Gorges area, South China, showing stratigraphic distribution of fossils and U–Pb radiometric ages. Star marks the stratigraphic occurrence of *Charnia* in the Shibantan limestone. Modified from S. Xiao et al. (2020) and Wu et al. (2021). Geochronometric data sources: Condon et al. (2005) and Yang et al. (2021) for the lower Doushantuo Formation and Miaohe Member; Huang et al. (2020) and Zhang et al. (2022) for the Baimatuo Member; Okada et al. (2014) for the Cambrian Shuijingtuo Formation. Cry. = Cryogenian; Fm. = Formation; Mbr. = Member; Cam. = Cambrian.

Institute of Geology and Palaeontology, Chinese Academy of Sciences (NIGPAS), with NIGPAS museum catalog numbers (prefix NIGP-) provided for each specimen.

Systematic paleontology

Genus *Charnia* Ford, 1958, emended Dunn et al., 2019

Type species.—*Charnia masoni* Ford, 1958

Charnia masoni Ford, 1958, emended
Figure 2.1, 2.2

1958 *Charnia masoni* Ford, p. 212, pl. 13, fig. 1.
?1959 *Charnia* sp.; Glaessner, p. 1472, text-fig. 1b.
?1959 *Rangea*?; Glaessner in Glaessner and Daily, p. 387, pl. 46, fig. 2.
1961 *Charnia* sp.; Glaessner, p. 75, text-fig.
1962 *Charnia* sp.; Glaessner, p. 484, pl. 1, fig. 4 (non fig. 5).
1962 *Charnia masoni*; Ford, fig. 4 (non fig. 5).
1966 *Rangea grandis*; Glaessner and Wade, p. 616, pl. 100, fig. 5.
1973 *Glaessnerina grandis*; Germs, p. 5, fig. 1D.
1976 *Charnia* ex gr. *masoni*; Sokolov, p. 141, text-fig.
1977 *Charnia* ex gr. *masoni*; Sokolov, p. 441.
1978 *Charnia* sp.; Fedonkin, fig. 3 (9).
1979 *Charnia masoni*; Glaessner, p. A99, fig. 12 (3).
1981a *Charnia masoni*; Fedonkin, p. 66, pl. 3, figs. 5, 6, pl. 29, fig. 1.
1981a *Zolotytsia biserialis*; Fedonkin, p. 67, pl. 3, fig. 7.
1981b *Charnia masoni*; Fedonkin, p. 100.
1981 *Charnia masoni*; Sokolov and Brekhovskikh, p. 3, text-fig.
1981 *Glaessnerina grandis*; Glaessner and Walter, fig. 6.11C.
1983a *Charnia masoni*; Fedonkin, pl. 1, fig. 1.
1983b *Charnia masoni*; Fedonkin, fig. 37.
1983 *Charnia masoni*; Sokolov and Fedonkin, p. 13, fig. 9.
1984 *Charnia masoni*; Sokolov, p. 6, text-fig.
1984 *Charnia masoni*; Sokolov and Fedonkin, fig. 3f.

https://doi.org/10.1017/jpa.2022.97 Published online by Cambridge University Press

Table 1. Biometric data for morphology comparison of *Charnia* specimens from the Shibantan biota and other localities.

	Petalodium		Longest first-order branch								
Locality	Length (mm)	Width (mm)	Length (mm)	Width (mm)	L/W Ratio	Largest width of constituent second-order branch (mm)	Range of divergence angle (°)	Mean divergence angle (°)	Mean X [=|(a − b)/(a + b)|]	Holdfast area (mm^2)	References
Charnwood Forest, UK	26.2	9.9	15.6	3.8	4.1	1.3	22.8~32.8	28.0	0.60	N/A	Dunn et al., 2021; fig. S2A; GSM 105994
	45.3	15.0	22.3	4.7	4.8	2.0	30.3~34.6	33.5	0.45	N/A	Dunn et al., 2021; fig. S2B; GSM 106084
	126.4	36.3	38.9	8.3	4.7	3.2	32.2~40.3	36.9	0.58	N/A	Dunn et al., 2019; fig. 3A; BGS GSM 106078
	179.8	63.2	60.2	15.3	3.9	4.6	40.4~46.1	44.0	1.32	N/A	Dunn et al., 2019; fig. 3C; BGS GSM 105997
	93.9	19.7	30.6	7.6	4.0	2.0	24.9~37.4	33.2	1.11	95.6	Dunn et al., 2019; fig. 5A; BGS GSM 105989
	168.6	43.5	57.0	10.9	5.2	4.1	27.4~36.1	32.0	0.73	N/A	Dunn et al., 2018; fig. 1E; LEIUG 2328
	440.1	104.4	120.2	23.9	5.0	6.6	38.0~46.0	39.8	1.41	N/A	Wilby et al., 2015; fig. 5.2; BGS GSM 105873
	92.8	23.6	33.0	6.2	5.3	2.0	28.1~37.3	27.6	0.79	N/A	Wilby et al., 2015; fig. 5.5; BGS GSM 105979
	82.3	20.3	28.7	5.5	5.3	2.1	23.0~27.9	26.1	0.86	N/A	Kenchington et al., 2018; fig. 1D; GSM105979
Newfoundland, Canada	135.8	17.7	40.0	5.5	7.3	3.2	18.4~25.9	24.2	0.75	96.8	Dunn et al., 2019; fig. 8A; CAMSM X.50297.5
	99.4	19.7	40.5	7.2	5.6	3.1	17.2~28.4	22.8	0.96	169.7	Dunn et al., 2019; fig. 8B; CAMSM X.50297.4
	108.3	14.8	24.9	5.9	4.2	2.2	23.2~27.8	25.5	N/A	555.9	Dunn et al., 2019; fig. 7A; CAMSM X.50297.10
	105.3	23.3	30.4	7.3	4.1	2.9	29.8~42.0	36.5	0.41	190.4	Dunn et al., 2019; fig. 7D; CAMSM X.50297.1
	122.1	30.4	47.0	8.5	5.5	3.4	14.9~37.6	26.2	0.55	N/A	Dunn et al., 2019; fig. 7E
	65.6	11.8	23.0	5.1	4.5	2.5	18.0~34.3	24.1	0.69	217.6	Liu et al., 2015; fig. 2D
	15.3	3.4	9.7	3.6	2.7	1.8	18.7~26.2	22.4	N/A	N/A	Liu et al., 2013; fig. 1d
	49.9	14.2	21.9	4.4	4.9	1.5	21.0~28.9	24.8	1.21	N/A	Hofmann et al., 2008; fig. 13. 1; NFM F-487
	90.1	15.8	21.3	5.7	3.7	2.4	29.4~39.9	32.7	0.55	106.7	Laflamme et al., 2007; fig. 4c
	58.5	13.9	24.4	4.3	5.7	1.8	23.7~30.3	27.8	0.82	19.8	Laflamme et al., 2007; fig. 4d
	65.2	18.8	27.1	6.8	4.0	1.7	25.5~34.3	29.6	0.42	N/A	Laflamme et al., 2007; fig. 4e
	116.2	30.4	49.2	10.8	4.5	4.9	13.1~28.0	22.4	0.56	N/A	Laflamme et al., 2007; fig. 4f
	119.3	28.5	44.9	10.0	4.5	3.8	24.9~28.9	27.3	0.50	N/A	Laflamme et al., 2007; fig. 4g
	92.2	15.9	29.3	8.6	3.4	3.8	31.7~39.3	35.6	0.37	145.5	Laflamme et al., 2007; fig. 4h
	203.3	37.2	57.9	12.8	4.5	5.6	22.8~27.6	25.2	0.93	N/A	Laflamme et al., 2007; fig. 4i
	39.0	11.5	20.2	5.1	4.0	2.3	26.6~36.9	31.4	0.50	34.9	Laflamme et al., 2007; fig. 4j
Sekwi Brook, NW Canada	N/A	16.2	14.0	4.2	3.3	1.0	39.0~46.5	43.3	N/A	N/A	Narbonne et al., 2014; fig. 53; ROM 62456
White Sea region, Russia	N/A	N/A	48.8	6.1	8.0	3.0	17.9~19.1	18.5	0.24	N/A	Fedonkin et al., 2007; fig. 232
	N/A	84.8	90.4	11.6	7.8	6.1	17.4~28.0	21.7	0.56	N/A	Martin et al., 2000; fig. 4A
	N/A	29.8	50.5	8.0	6.3	4.2	22.0~27.6	24.5	0.60	1,020.7	Grazhdankin and Bronnikov, 1997; fig. 2d; PIN no. 4717-3
	N/A	65.3	118.5	20.4	5.8	6.6	21.4~31.4	27.8	0.56	N/A	Sokolov and Fedonkin, 1984; fig. 3f
Flinders Ranges, South Australia	N/A	60.4	72.3	8.9	8.1	3.7	24.2~30.8	27.3	0.75	N/A	Gehling and Droser, 2013; fig. 2Q
	N/A	76.0	58.1	18.2	3.2	7.0	33.3~49.1	40.2	0.58	N/A	Germs, 1973; fig. 1D
Olenek Uplift, Siberia	163.3	29.1	65.2	6.9	9.4	4.9	17.7~22.3	19.8	0.17	N/A	Grazhdankin et al., 2008; fig. 2A
	N/A	53.8	46.8	9.0	5.2	3.8	39.2~52.1	45.2	0.84	N/A	Runnegar and Fedonkin, 1992; fig. 7.5.5 A; PIN no. 3995/125

Yangtze Gorges area, South China	73.3	12.2	24.5	3.4	7.2	2.4	11.9~17.9	14.4	0.11	N/A	This study; Fig. 2.6; NIGP161631
	138.0*	23.4	38.0	5.0	7.5	2.8	14.2~20.4	17.7	0.25	N/A	This study; not illustrated
	172.3	20.5	54.2	3.7	14.7	2.8	11.6~17.7	14.9	0.23	N/A	This study; Fig. 2.4; NIGP161629
	555.7*	73.1	164.8	8.5	19.4	4.7	9.1~16.7	11.6	0.15	N/A	This study; Fig. 3.1; NIGP161634
	178.7*	58.2	76.3	8.0	9.6	4.4	15.2~16.5	15.9	N/A	N/A	This study; not illustrated
	92.1	14.8	31.0	3.7	8.5	2.2	12.5~19.4	15.9	0.22	N/A	This study; Fig. 2.5; NIGP161630
	81.0*	16.0	30.3	4.1	7.5	2.3	12.9~21.4	16.7	0.16	N/A	This study; Fig. 2.8; NIGP161633
	70.0*	14.6	31.9	3.2	9.8	2.3	10.2~21.3	14.8	0.25	40.4	This study; Fig. 2.7; NIGP161632
	72.4	10.7	24.3	3.8	6.4	1.2	11.0~21.7	16.3	0.08	N/A	This study; Fig. 3.4; NIGP161635
	251.5*	113.5	103.1	11.8	8.8	5.1	23.3~45.4	34.0	N/A	6,261.2	This study; Fig. 2.1; NIGP161628
Oulongbuluke terrane, Qaidam, NW China	28.5	4.7	6.4	1.4	4.7	0.5	17.7~39.6	27.7	N/A	N/A	Pang et al., 2021; fig. 3A; NIGP161610
	21.5	9.0	13.0	2.9	4.5	1.2	13.0~25.2	21.9	0.46	N/A	Pang et al., 2021; fig. 3B; NIGP161611
	N/A	N/A	13.8	2.7	5.1	2.0	20.9~30.3	26.9	N/A	N/A	Pang et al., 2021; fig. S2B; NIGP161616
	N/A	N/A	15.4	2.7	5.8	N/A	25.4~28.2	26.7	N/A	N/A	Pang et al., 2021; fig. S2C; NIGP161617
	N/A	13.4	18.2	4.5	4.1	N/A	21.8~36.7	28.4	N/A	N/A	Pang et al., 2021; unpublished

*Incomplete petalodium.

1984 *Charnia* cf. *C. masoni*; Glaessner, fig. 2.21B.
1984 *Charnia masoni*; Glaessner, fig. 2.21A.
1984 *Glaessnerina grandis*; Glaessner, fig. 2.21C.
1985 *Charnia masoni*; Fedonkin, p. 99, pl. 12, fig. 4, pl. 13, figs. 2–4.
1985 *Charnia* cf. *C. masoni*; Jenkins, fig. 7C.
1985 *Charnia masoni*; Jenkins, fig. 7B.
1987 *Charnia masoni*; Fedonkin, pl. 15.
1987 *Glaessnerina grandis*; Preiss, fig. E.
1990 *Charnia masoni*; Fedonkin, p. 110, pl. 12, fig. 4, pl. 13, figs. 2–4.
1992 *Charnia masoni*; Fedonkin, figs. 28–30.
1992 *Charnia masoni*; Runnegar and Fedonkin, fig. 7.5.5A, 7.5.10A.
1994 *Charnia masoni*; Fedonkin, fig. 2A, B.
1995 *Charnia grandis*; Boynton and Ford, p. 168, fig. 1.
1996 *Glaessnerina grandis*; Jenkins, p. 35, fig. 4.1.
1997 *Charnia masoni*; Grazhdankin and Bronnikov, fig. 2a, d.
1999 *Charnia grandis*; Ford, p. 231, figs. 1, 3.
2000 *Charnia*; Martin et al., fig. 4A.
2004 *Charnia*; Grazhdankin, fig. 2.
2004 *Charnia*-like frond; Narbonne, fig. 3D.
2005 *Charnia masoni*; Narbonne et al., pl. 1L.
2005 *Charnia*; Grazhdankin et al., fig. 3d.
2007 *Charnia masoni*; Laflamme et al., p. 252, fig. 4A–J.
2007 *Charnia* cf. *C. masoni*; Fedonkin et al., fig. 276 (partim).
2007 *Charnia* cf. *C. masoni*; Fedonkin et al., figs. 304, 314 (partim).
2007 *Charnia masoni*; Fedonkin et al., p. 265, fig. 354.
2008 *Charnia masoni*; Hofmann et al., p. 16, fig. 13.1, 13.2.
2008 *Charnia grandis*?; Hofmann et al., p. 16, fig. 14.
2009 *Charnia masoni*; Bamforth and Narbonne, fig. 7.5.
2011 *Charnia masoni*; Wilby et al., figs. 2A, 3A.
2011 *Charnia masoni*; Grazhdankin, fig. 3a–d.
2012 *Charnia masoni*; Liu et al., figs. 4b, 5a.
2012 *Charnia* aff. *C. masoni*; Liu et al., fig. 4a.
2013 *Charnia* aff. *C. masoni*; Liu et al., fig. 1d.
2013 *Charnia masoni*; Liu et al., fig. 2a–d.
2013 *Charnia* sp.; Gehling and Droser, fig. 2Q.
2014 *Charnia* cf. *C. masoni*; Narbonne et al., p. 215, fig. 5.1–5.4.
2015 *Charnia masoni*; Noble et al., fig. 4A, G.
2015 *Charnia masoni*; Wilby et al., fig. 5.
2015 *Charnia masoni*; Liu et al., fig. 2D.
2016 *Charnia masoni*; Liu et al., fig. 3D.
2017 *Charnia masoni*; Antcliffe et al., fig. 4E.
2018 *Charnia masoni*; Dunn et al., figs. 1E, 3.
2018 *Charnia masoni*; Kenchington et al., figs. 1A, D, 7E (partim).
2019 *Charnia masoni*; Dunn et al., p. 16, figs. 1–3, 5–8, 10.
2020 *Charnia masoni*; Liu and Dunn, fig. 4d.
2021 *Charnia masoni*; Matthews et al., fig. 2B.
2021 *Charnia masoni*; McIlroy et al., fig. 1b.
2021 *Charnia masoni*; Pang et al., figs. 3A–C, S2A–E.
2021 *Charnia masoni*; Dunn et al., figs. 1 (A-2), S1–S2.
2022 *Charnia masoni*; Butterfield, figs. 1a, 2.
2022 *Charnia masoni*; McIlroy et al., fig. 10f.

Holotype.—LEIUG 2328, from Bed B (Wilby et al., 2011), North Quarry, Charnwood Forest, UK.

https://doi.org/10.1017/jpa.2022.97 Published online by Cambridge University Press

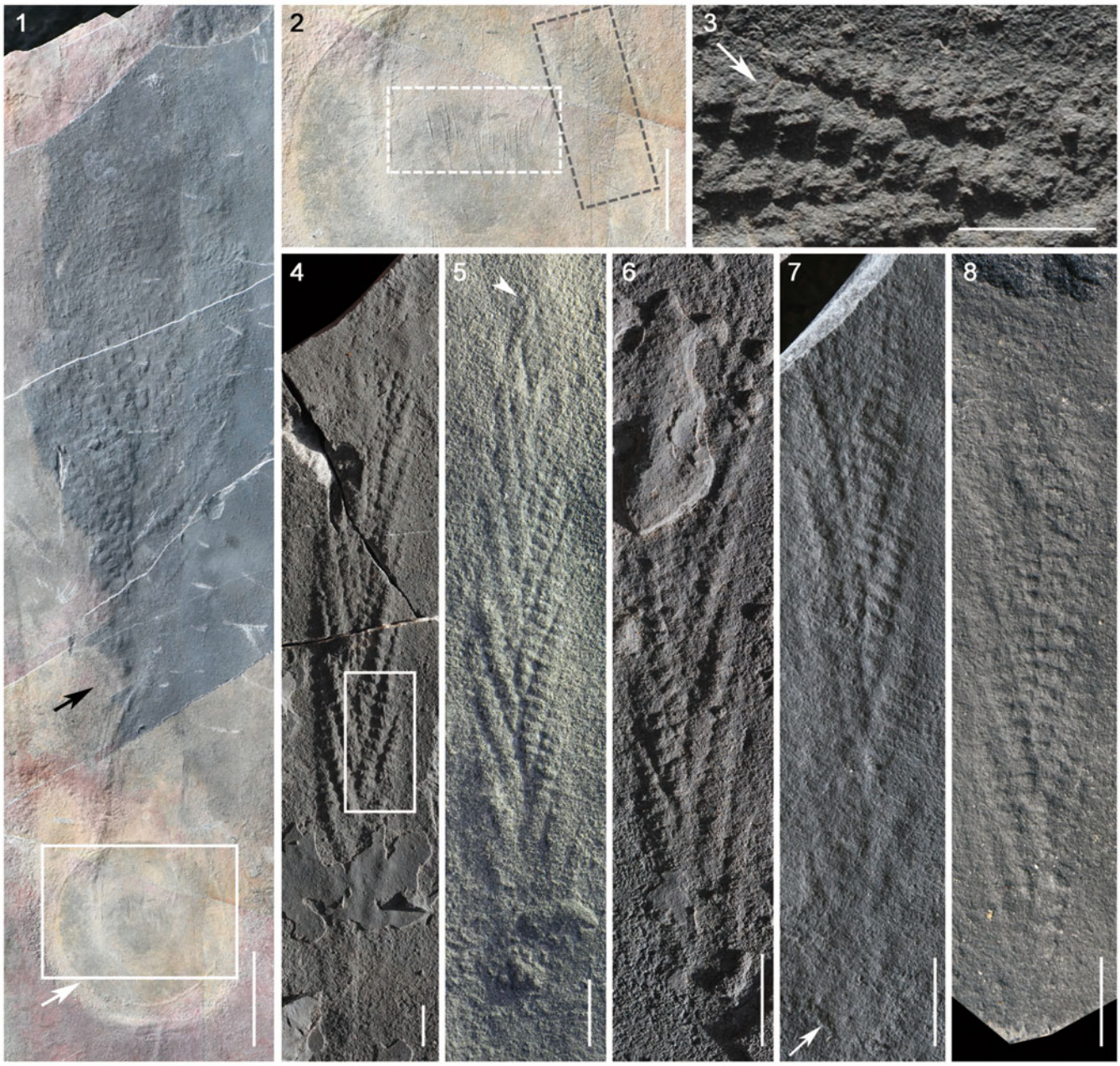

Figure 2. (**1**) *Charnia masoni* from the Shibantan limestone preserved in positive relief, bed sole view; black arrow points to twisted stem and white arrow points to discoidal holdfast; (**2**) magnified view of rectangle in (**1**), with black and white rectangles marking two different orientations of filiform structures on the holdfast; NIGP161628. (**3, 4**) Holotype of *C. gracilis* n. sp. from the Shibantan limestone preserved in positive relief, bed sole view: (**3**) magnified view of rectangle in (**4**), showing well-preserved second-order branches and possible third-order branches (arrow); note the straight first-order branches with small divergence angles in (**4**); NIGP161629. (**5**) Specimen of *C. gracilis* n. sp. with complete petalodium, preserved in positive relief, bed sole view; arrowhead points to apex of petalodium; NIGP161630. (**6**) Specimen of *C. gracilis* n. sp. preserved in positive relief, bed sole view; NIGP161631. (**7**) Incomplete specimen of *C. gracilis* n. sp. preserved in positive relief, bed sole view; arrow points to a possible and faintly preserved holdfast; NIGP161632. (**8**) Incomplete specimen of *C. gracilis* n. sp. preserved in positive relief, bed sole view; NIGP161633. (**1**) Scale bar = 5 cm; (**2**) scale bar = 2 cm; (**3–8**) scale bars = 1 cm.

Emended diagnosis.—*Charnia* with ovate to parallel-sided petalodium consisting of sigmoidal first-order branches emanating alternately at an acute angle, typically >20°. First-order branches composed of series of near-rectangular second-order branches arranged acutely to almost perpendicularly to the first-order branches.

Occurrence.—Shibantan Member, Dengying Formation, Yangtze Gorges area, South China (S. Xiao et al., 2020); Bradgate Formation, Charnian Subgroup, Charnwood Forest, UK (Wilby et al., 2011); Drook, Briscal, Mistaken Point, Trepassey, and Fermeuse formations, Newfoundland, Canada (Narbonne, 2004; Laflamme et al., 2007; Hofmann et al., 2008; Liu et al., 2012; Dunn et al., 2019; Matthews et al., 2021); Nadaleen Formation (previously known as "June Beds," Moynihan et al., 2019), northwestern Canada (Narbonne et al., 2014); Khatyspyt Formation, Olenek Uplift, north-central Siberia, Russia (Grazhdankin et al., 2008);

https://doi.org/10.1017/jpa.2022.97 Published online by Cambridge University Press

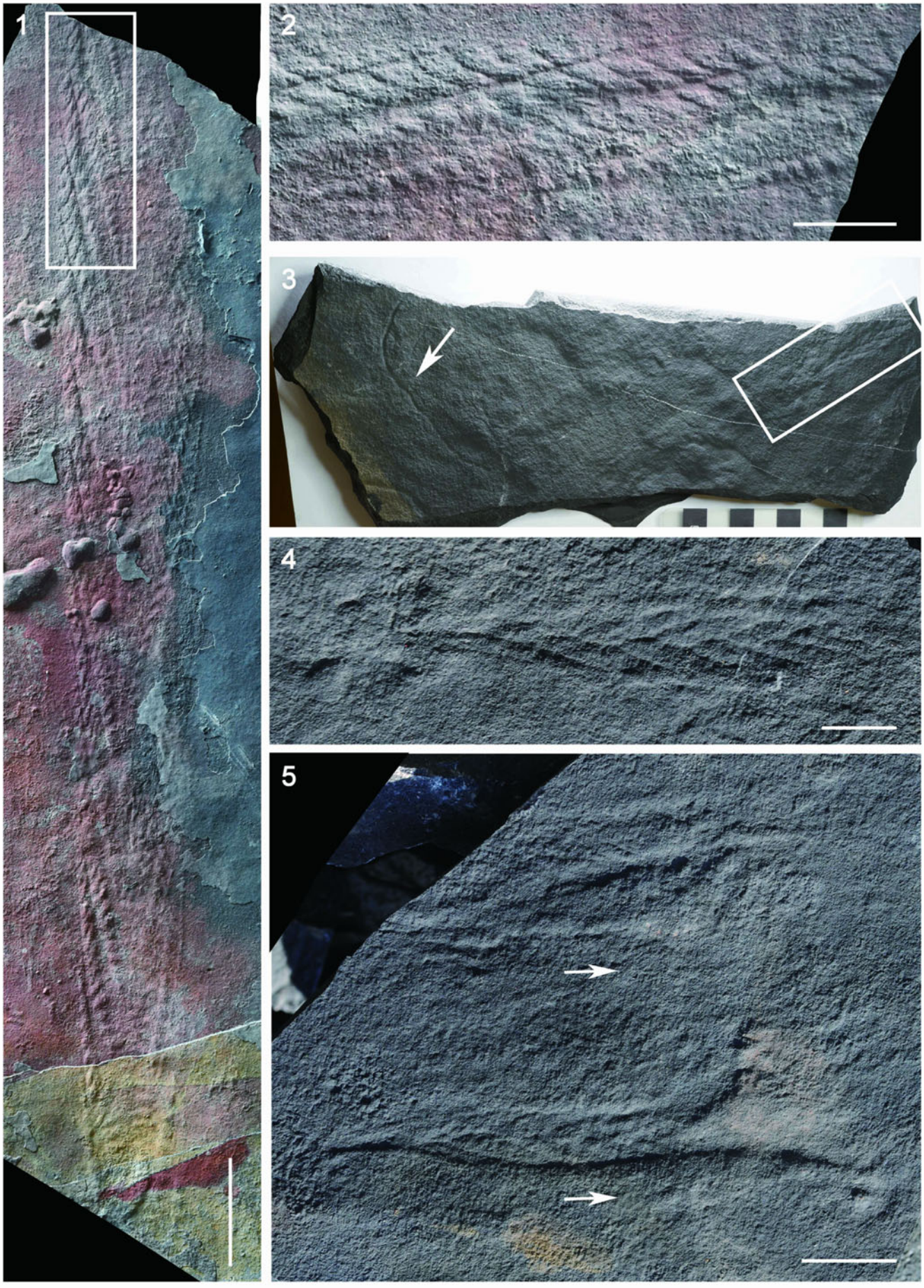

https://doi.org/10.1017/jpa.2022.97 Published online by Cambridge University Press

Figure 3. *Charnia gracilis* new species from the Shibantan limestone. (**1, 2**) The longest specimen of *C. gracilis* n. sp. in the Shibantan limestone with an incomplete petalodium and well-preserved second-order branches, positive relief, bed sole view; (**2**) magnified view of the rectangle in (**1**), showing rhomboidal second-order branches and inclined third-order branches; NIGP161634. (**3, 4**) A juvenile specimen of *C. gracilis* n. sp. marked by rectangle in (**3**), positive relief, bed sole view; the specimen is preserved together with a *Helminthoidichnites*-like trace fossil, marked by arrow in (**3**); (**4**) magnified view of rectangle in (**3**); NIGP161635. (**5**) A possible juvenile specimen of *C. gracilis* n. sp. (bottom) and another poorly preserved unnamed frond (upper) preserved in positive relief, bed sole view. Arrows point to inferred direction of water current that felled and aligned the specimens. NIGP161636. (**1**) Scale bar = 5 cm; (**2, 5**) scale bars = 2 cm; (**3, 4**) scale bars = 1 cm.

Verkhovka Formation, the White Sea region, Russia (Martin et al., 2000); Rawnsley Quartzite, Flinders Ranges, South Australia (Gehling and Droser, 2013).

Description.—Only one specimen in our collections can be assigned to this species. The specimen is characterized by a uniterminal bifoliate frond comprising an incompletely preserved ovate petalodium connected to a discoidal holdfast at the basal end by a stem (Fig. 2.1). The incomplete petalodium is 113.5 mm wide, and its preserved length is 251.5 mm. Petalodium is composed of strongly constrained (sensu Narbonne et al., 2009) first-order branches (sensu Dunn et al., 2021) or primary branches, which emanate alternately on each side of the zig-zag central axis at an angle of 23.3–45.4° (mean = 34.0°). The longest first-order branch is 103.1 mm long and 11.8 mm wide. First-order branches are inclined toward the apex of the frond and are more or less sigmoidal in shape. First-order branches at the apical end of the petalodium are poorly preserved but seem to be shorter than those at the proximal end. First-order branches appear to be rotated and furled (sensu Brasier et al., 2012) or single-sided (sensu Narbonne et al., 2009). First-order branches are composed of about a dozen rectangular to near-rectangular second-order branches (sensu Dunn et al., 2021) or secondary branches. Second-order branches in the longest first-order branch of each specimen are 4.3–5.1 mm (mean = 4.7 mm, n = 5) wide and arranged perpendicularly to the first-order branch. Third-order branches (sensu Dunn et al., 2021) are not observed. The stem is twisted and 158.8 mm long (measured from the base of petalodium to the center of the holdfast). The holdfast is discoidal, 87.7 mm in diameter, with a few filiform-texture structures in the middle (Fig. 2.2).

Materials.—One specimen (NIGP161628) from Shibantan Member, Dengying Formation at Wuhe quarry.

Remarks.—Three species of the genus *Charnia*—*Charnia grandis* Glaessner and Wade, 1966, *Charnia wardi* Narbonne and Gehling, 2003, and *Charnia antecedens* Laflamme et al., 2007—have previously been erected in addition to its type species *Charnia masoni* Ford, 1958. However, *C. grandis* is considered a junior synonym of *C. masoni* (Wilby et al., 2011; Brasier et al., 2012), whereas *C. wardi* and *C. antecedens* were subsequently reassigned to *Trepassia* Narbonne et al., 2009 and *Vinlandia* Brasier et al., 2012, respectively. This Shibantan specimen is tentatively classified in the genus *Charnia* due to its constrained and alternately arranged first-order branches as well as its single-sided rangeomorph units. The divergence angle of first-order branches of this specimen, 34.0° on average, is similar to that of the *C. masoni* specimens from other localities and much larger than that of the other Shibantan *Charnia* specimens (Table 1). First-order branches of this specimen are more curved than those of the other Shibantan *Charnia* specimens (Table 1). Its ovate petalodium and sigmoidal first-order branches also share similarities with other *C. masoni* specimens elsewhere. Taking all these factors into account, we choose to assign this specimen to *C. masoni*.

This specimen bears a twisted stem and a relatively large holdfast (Fig. 2.1), which are rare in previously reported *Charnia* specimens. The stem, together with the proximal end of the petalodium, seems to have been affected by water currents. The holdfast bears filiform textures in the middle (Fig. 2.2), somewhat different from *Hiemalora*-like holdfasts, which have radially arranged tentacle-like structures around the rim of the central disc (e.g., Chen et al., 2014, fig. 4; Shao et al., 2019, fig. 2). The filiform textures could represent drag structures generated by uprooting of the holdfast (Tarhan et al., 2010), consistent with the twisting of the stem. However, there seem to be at least two sets of filiform textures that are perpendicular to each other, an observation not easily accounted for by uprooting. Alternatively, the filiform textures may be wrinkles resulting from the compression of an originally three-dimensional bulbous holdfast. They are also broadly similar to the radial and concentric bands and filamentous mesh present in an *Ediacaria* disc from the White Sea region, which was interpreted as possible "skeletal" structure by Luzhnaya and Ivantsov (2019).

Charnia gracilis new species
Figures 2.3–2.8, 3

?1972a *Rangea sibirica*; Sokolov, p. 50.
?1972b *Rangea sibirica*; Sokolov, pl. 1, fig. 3.
?1979 *Glaessnerina sibirica*; Glaessner, p. A99, fig. 12 (1).
?1984 *Glaessnerina sibirica*; Glaessner, fig. 2.21D.
?1998 *Charnia masoni*; Nedin and Jenkins, p. 315, fig. 1.
2007 *Charnia* sp.; Fedonkin et al., fig. 232 (partim).
2008 *Charnia masoni*; Grazhdankin et al., fig. 2A.
2014 *Charnia masoni*; Grazhdankin, fig. 2.3.
2020 *Charnia* sp.; S. Xiao et al., fig. 4f.

Holotype.—NIGP161629, from Shibantan Member, Dengying Formation, Yangtze Gorges area, South China, illustrated in Fig. 2.4.

Diagnosis.—A *Charnia* species characterized by a slender petalodium consisting of relatively long, thin, and straight first-order branches that have a parallel-sided blade-like shape. First-order branches emanate alternately from the central axis at an acute angle, typically ≤20°. First-order branches are composed of a series of rectangular or rhomboid second-order branches arranged acutely to perpendicularly to the first-order branches.

https://doi.org/10.1017/jpa.2022.97 Published online by Cambridge University Press

Occurrence.—Shibantan Member, Dengying Formation, Yangtze Gorges area, South China; Khatyspyt Formation, Olenek Uplift, north-central Siberia, Russia (Grazhdankin et al., 2008); Verkhovka Formation, the White Sea region, Russia (Fedonkin et al., 2007); possible occurrence in Rawnsley Quartzite, Flinders Ranges, South Australia (Nedin and Jenkins, 1998).

Description.—Specimens are characterized by a centimeter- to decimeter-scale, uniterminal bifoliate frond comprising a nearly parallel-sided and spicate petalodium tapering gradually at the apical end (Figs. 2.3–2.8, 3). There are four specimens in our collection that bear a completely preserved petalodium, which is 72.4–172.3 mm long (mean = 102.5 mm, n = 4) and 10.7–20.5 mm wide (mean = 14.6 mm, n = 4). Incomplete petalodia of five other specimens can be measured for maximum width, which varies from 14.6 mm to 73.1 mm (mean = 37.0 mm, n = 5), and their preserved length varies from 70.0 mm to 555.7 mm (mean = 204.7 mm, n = 5). Two additional specimens are too incompletely or poorly preserved to allow reliable measurements of petalodium width and length; thus, they are not included in the measurement data. The petalodium is composed of about a dozen strongly constrained (sensu Narbonne et al., 2009) first-order branches (sensu Dunn et al., 2021). First-order branches emanate alternately on each side of the central axis at an angle of 9.1–21.7°, with the average divergence angle (11.6–17.7° for nine specimens) usually <20°. Opposing first-order branches are offset by half a branch width, forming a zig-zag central suture (e.g., Fig. 2.4). First-order branches are inclined toward the apex of the frond and are nearly straight, although they can be slightly curved at both proximal and distal ends, leading to a blade-like shape. Proximal first-order branches are usually more curved than distal ones. The longest first-order branch usually occurs near the middle of the petalodium, 24.3–164.8 mm long (mean = 52.8 mm, n = 9) and 3.3–8.5 mm wide (mean = 4.8 mm, n = 9). First-order branches are composed of about a dozen second-order branches (sensu Dunn et al., 2021) arranged parallel to one another. The widest second-order branches in the longest first-order branch are 1.2–4.7 mm (mean = 2.8 mm, n = 9) wide. Second-order branches vary in shape and orientation in specimens of different sizes. In smaller specimens (e.g., Fig. 2.3–2.8), second-order branches are generally near rectangular and arranged more or less perpendicularly to the first-order branch, whereas in larger specimens (e.g., Fig. 3.1, 3.2), second-order branches are rhomboidal and arranged more acutely to the first-order branch. The number of second-order branches in each first-order branch seems to remain more or less constant (Fig. 4.1), whereas the average size of second-order branches in each first-order branch increases by ~14 times as the length of the first-order branch increases ~eight times (Fig. 4.2). The shape of second-order branches can also vary from rectangular or rhomboidal in the central region to trigonal or trapezoidal in the proximal and distal regions of the first-order branch (e.g., Fig. 2.3). Rangeomorph units of both first-order branches and second-order branches are rotated and furled (sensu Brasier et al., 2012) or single-sided (sensu Narbonne et al., 2009). Third-order branches (sensu Dunn et al., 2021) are barely discernable in some second-order branches, characterized by obliquely arranged ridges (e.g., Figs. 2.3, 3.2). First-order and third-order branches are inclined toward the apex of the frond. A discoidal holdfast is faintly preserved in one specimen (Fig. 2.7), ~7.3 mm in diameter. A *Charnia*

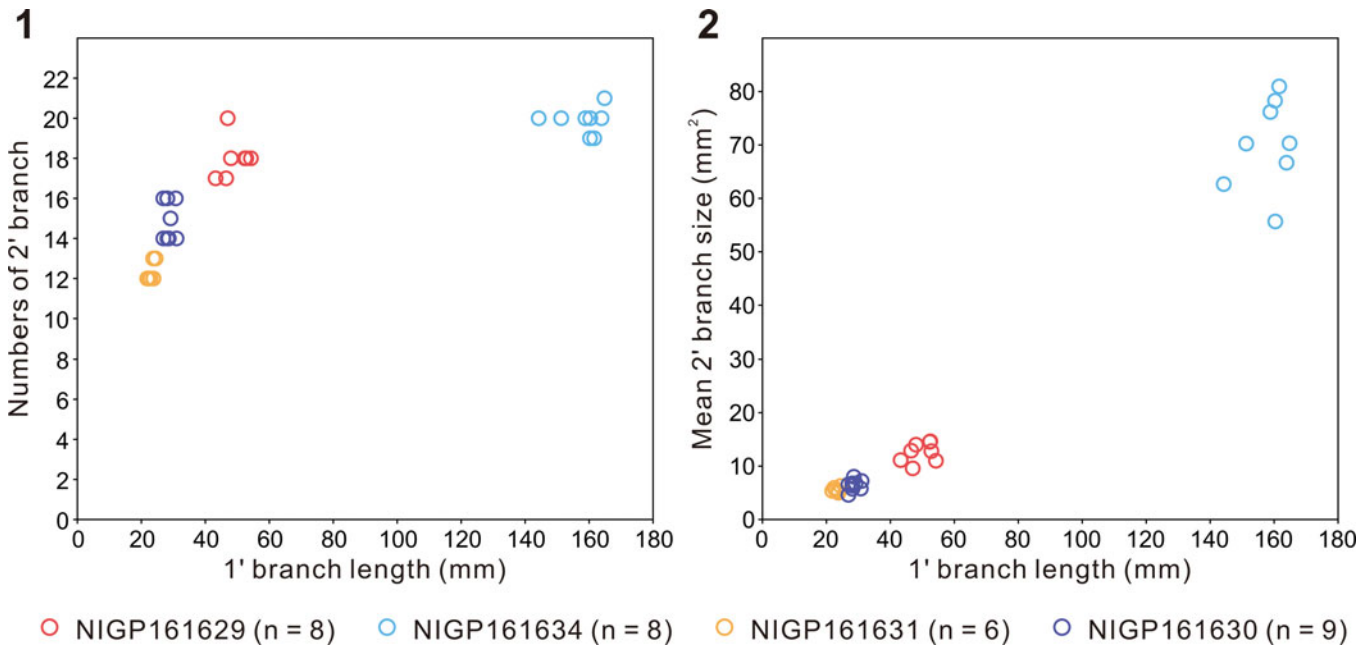

Figure 4. Measurements of several specimens of *Charnia gracilis* new species with well-preserved second-order branches (NIGP161629; NIGP161630; NIGP161631; NIGP161634). (**1**) Cross-plot of first-order branch (1' branch) length versus number of constituent second-order branches (2' branches); (**2**) Cross-plot of first-order branch length versus average size of constituent second-order branches. The number of second-order branches in each first-order branch is evaluated by dividing the length of the first-order branch by the average width of constituent second-order branches that are measurable.

https://doi.org/10.1017/jpa.2022.97 Published online by Cambridge University Press

gracilis n. sp. specimen (Fig. 3.4) is preserved together with a *Helminthoidichnites*-like trace fossil on the same bedding surface (Fig. 3.3). A possible juvenile specimen of *C. gracilis* is in alignment with another poorly preserved, taxonomically unidentifiable frond (Fig. 3.5), indicating common orientation of tethered, erect epibenthic organisms by water currents.

Etymology.—From *gracilis* (Latin, slender), in reference to the slender shape of the petalodium as well as the first-order branches.

Materials.—Eleven specimens in total, from Shibantan Member, Dengying Formation at Wuhe quarry.

Remarks.—The Shibantan specimens possess diagnostic features of the genus *Charnia*, including single-sided rangeomorph units, strongly constrained first-order branches, and a zig-zag midline. Biometric plots also show that these Shibantan specimens share similarities with *Charnia* specimens from other localities (Fig. 5; Table 1). For example, the petalodium length versus width (Fig. 5.1), as well as the width of the longest first-order branch versus the largest width of second-order branch in the longest first-order branch (Fig. 5.2), is similar between the Shibantan specimens and *C. masoni* from Charnwood Forest, UK (Wilby et al., 2015; Dunn et al., 2018, 2019, 2021), *C. masoni* from Newfoundland, Canada (Laflamme et al., 2007; Hofmann et al., 2008; Liu et al., 2013, 2015), *Charnia* cf. *C. masoni* from Sekwi Brook, NW Canada (Narbonne et al., 2014), *C. masoni* and *C. gracilis* n. sp. from the White Sea region, Russia (Sokolov and Fedonkin, 1984; Grazhdankin and Bronnikov, 1997; Martin et al., 2000), *C. masoni* from Flinders Ranges, South Australia (Germs, 1973; Gehling and Droser, 2013), *C. masoni* and *C. gracilis* from Olenek Uplift, Siberia (Runnegar and Fedonkin, 1992; Grazhdankin et al., 2008), and *C. masoni* from Oulongbuluke terrane, NW China (Pang et al., 2021). Thus, it is reasonable to assign the Shibantan specimens to the genus *Charnia*. However, there are several notable differences between the Shibantan specimens and *C. masoni*. Relative to *C. masoni* specimens from other localities, the Shibantan specimens have first-order branches that are slenderer, longer, and straighter, taper more gradually toward the distal end, have a higher length/width ratio (Fig. 5.3, 5.4), and present a blade-like rather than a sigmoidal shape (Fig. 5.5, 5.9). In addition, the first-order branches are straight and blade-like in the Shibantan specimens but sigmoidal in *C. masoni*. This difference can be quantified using a new morphologic descriptor defined as $X = |(a - b)/(a + b)|$, where "a" and "b" are the angles between the diagonal line and borderlines at the distal end of first-order branches (Fig. 5.9). It can be shown that the parameter X effectively distinguishes the sigmoidal ($X \geq 0.3$ for *C. masoni*) or straight ($0 \leq X < 0.3$ for *C. gracilis*) first-order branches (Fig. 5.5). Finally, the mean divergence angle of the first-order branches in the Shibantan specimens, ranging between 12° and 18°, is much lower than in *C. masoni* specimens elsewhere (Fig. 5.4, 5.5). Considering these morphological disparities as likely interspecific variations, we choose to erect a new species, and we use the mean divergence angle of the first-order branches to differentiate *C. gracilis* (≤20°) and *C. masoni* (>20°).

Grazhdankin et al. (2008) reported *Charnia masoni* from the Khatyspyt Formation in Siberia (Grazhdankin et al., 2008, fig. 2A). Although incompletely preserved, this Khatyspyt specimen has straight and thin first-order branches with an average divergence angle of 19.8° (Fig. 5.4, 5.5; Table 1). This Khatyspyt specimen shares more morphological similarities with *C. gracilis* specimens from the Shibantan Member than typical *C. masoni* material; therefore, it is more appropriate to reassign this specimen to *C. gracilis*. An incompletely preserved *Charnia* sp. specimen from the White Sea region (Fedonkin et al., 2007, fig. 232) may also be considered *C. gracilis*. This incomplete specimen possesses a near-parallel-sided petalodium and relatively straight first-order branches with an average divergence angle of 18.5° (Fig. 5.4; Table 1). An incomplete *Charnia* specimen from Siberia (Glaessner, 1979, fig. 12.1), which was assigned to *Glaessnerina sibirica* (Sokolov, 1973), is similar to the Shibantan *C. gracilis* specimens in its thin, straight, and parallel-sided first-order branches. Its inclined second-order branches are similar to those of the longest specimen in Shibantan limestone (Fig. 3.1). However, the poor preservation of the middle and left parts of its petalodium makes measurement of the divergence angle of the first-order branches difficult. Therefore, this specimen can be only provisionally placed in *C. gracilis*. A *Charnia* specimen reported by Nedin and Jenkins (1998) from the Rawnsley Quartzite, South Australia, also resembles the Shibantan *C. gracilis* specimens in its straight, slender, and acutely divergent (17.5–26.1°) first-order branches, but its mean divergence angle (21.7°; $n = 5$) is slightly larger than those of the latter. In general, the *Charnia* specimens from the White Sea and Nama assemblages can be related to or even reassigned to *C. gracilis*, on the basis of the morphology of first-order branches, which are more acutely diverged, less curved, and apically thinner and straighter than those from the Avalon assemblage (e.g., Dunn et al., 2019, fig. 1F). However, *C. gracilis* is also somewhat similar to some specimens from Newfoundland in their parallel-sided outlines of the petalodium (e.g., Laflamme et al., 2007, fig. 4f–h; Liu et al., 2015, fig. 2D; Dunn et al., 2019, fig. 8A), despite the fact that their first-order branches are different (Fig. 5; Table 1).

Dunn et al. (2019) studied *Charnia masoni* specimens from different localities and found that they are comparable in morphology but hard to accord with the morphological reconstructions of some other rangeomorphs such as *Avalofractus* (Narbonne et al., 2009) and *Rangea* (Vickers-Rich et al., 2013), which possess an internal central stalk (also refer to Dunn et al., 2021, fig. 5). Some researchers envisioned that an internal stalk may also be present in *Charnia* (Narbonne et al., 2009), but subsequent studies by other researchers found no evidence for a central stalk (Dunn et al., 2019; see also Dunn et al., 2021, fig. 5). The Shibantan *C. gracilis* specimens, which are similar in overall morphology to *Charnia* fossils reported elsewhere, show no sign of a central stalk.

Discussion

The differences between *Charnia gracilis* n. sp. and *Charnia masoni* lie mainly in their first-order branches, as revealed by biometric analysis of *Charnia* specimens worldwide (Fig. 5).

https://doi.org/10.1017/jpa.2022.97 Published online by Cambridge University Press

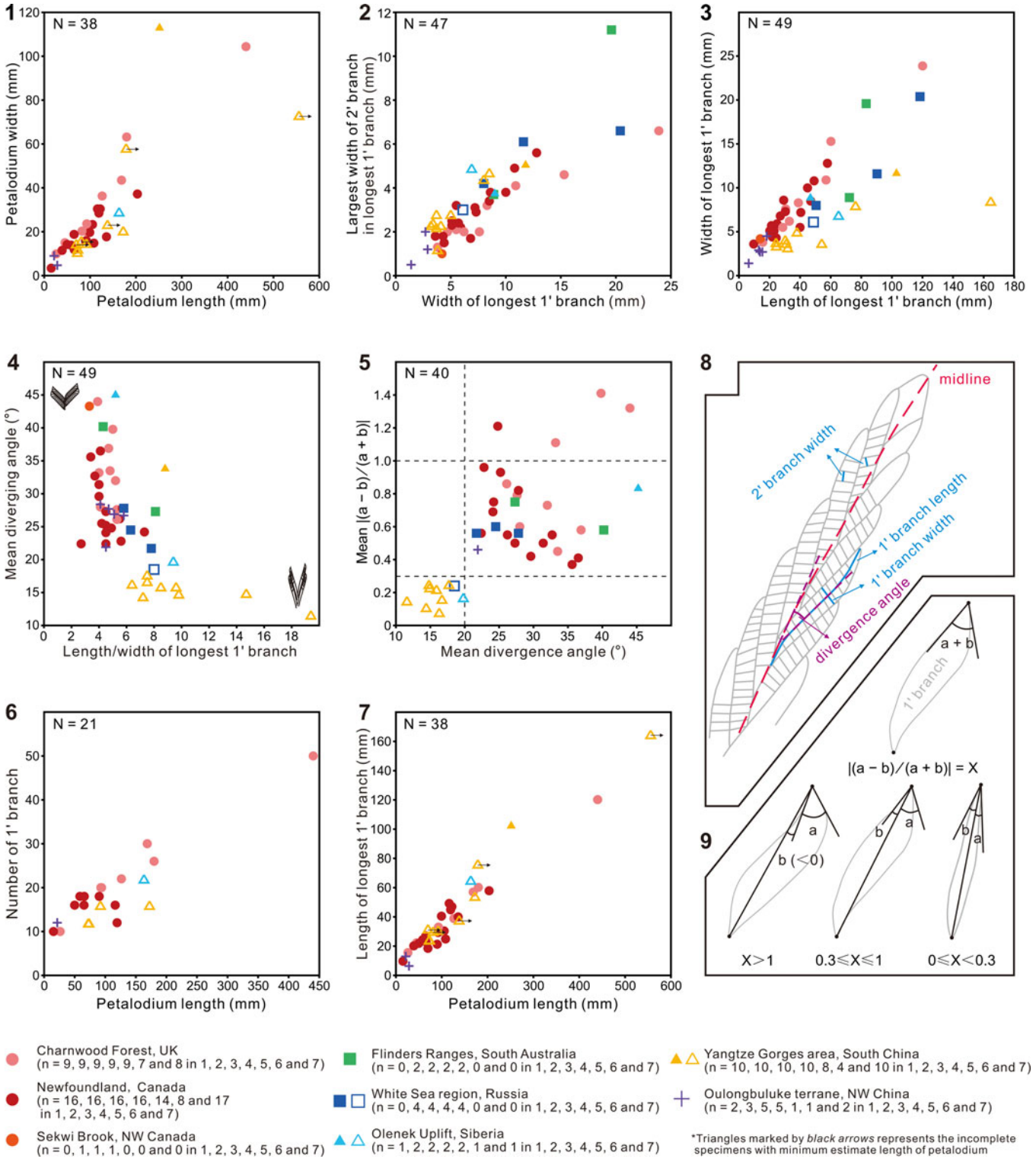

Figure 5. Biometric plots of *Charnia* from Shibantan limestone and other localities. (**1**) Cross-plot of petalodium length versus width. (**2**) Cross-plot of width of the longest first-order branch (1'branch) versus width of the widest second-order branch (2' branch) in the longest first-order branch. (**3**) Cross-plot of length versus width of the longest first-order branch. (**4**) Cross-plot of the length/width (L/W) ratio of the longest first-order branch versus mean divergence angle of first-order branches. Sketches at the lower right and upper left in (**4**) show first-order branches of two representative endmembers. (**5**) Cross-plot of mean divergence angle versus mean value of $X = |(a - b)/(a + b)|$; "a" and "b" represent the included angles between the diagonal line and borderlines at the distal end of first-order branches. (**6**) Cross-plot of petalodium length versus countable number of first-order branches. (**7**) Cross-plot of petalodium length versus length of the longest first-order branch. (**8**) Schematic diagram depicting how measurements for first- and second-order branches were made. (**9**) Schematic diagram depicting how measurements for $X = |(a - b)/(a + b)|$ were made to distinguish the sigmoidal or straight shape of the first-order branches; note that in the lower left case, angle "b" < 0 and angle "a" > 0 ($X > 1$), whereas in the two other lower cases, both angle "b" and angle "a" are ≥0 ($0 \leq X \leq 1$). Localities are represented by symbols with different colors and shapes. Triangles with an attached arrow represent specimens with incomplete petalodium length in (**1**) and (**7**). Dots represent the Avalon assemblage, squares represent the White Sea assemblage, and triangles and crosses represent younger assemblages, possibly belonging to the Nama assemblage. Hollow symbols represent measurements of *C. gracilis* new species, whereas filled symbols represent measurements of other *Charnia* species.

https://doi.org/10.1017/jpa.2022.97 Published online by Cambridge University Press

The Shibantan specimens of *C. gracilis* show notable differences from *Charnia* specimens elsewhere, with a straight blade-like shape, lower divergence angles, and greater length/width ratios for their first-order branches (Fig. 5.4, 5.5). These differences are unlikely to be artifacts of tectonic or taphonomic deformation. Tectonic shearing can be ruled out because associated holdfast structures are perfectly circular in shape (Fig. 3.2). Although taphonomic deformation did occur in some Shibantan fossils (e.g., *Dickinsonia*, Wang et al., 2021; see also slightly C-shaped fronds in Fig. 3.5), the tightly constrained first-order branches (Narbonne et al., 2009) in *C. gracilis* left little room for their postmortem dislocation, rotation, or deformation. Postmortem compression or stretching of the petalodium, which would increase the length/width ratio of the petalodium, straighten the first-order branches, and decrease their divergence angles, also seemed unlikely to have happened in such a uniform fashion simultaneously.

In addition to the shape of first-order branches of *Charnia gracilis* specimens, it is unlikely that their lower divergence angles result from alignment by strong currents. Some Shibantan *Charnia* specimens do show evidence of alignment (Fig. 3.5), perhaps by water currents, although there is no sedimentary evidence for strong water currents in the fossil-bearing horizons (Chen et al., 2014; Duda et al., 2016). It is conceivable that the lower divergence angles of *C. gracilis* specimens may be a biostratinomic artifact related to deformation by strong currents, but this interpretation contradicts the observation that the Shibantan *C. masoni* specimen, which has a twisted stem and a wrinkled holdfast that may be caused by water currents (Fig. 2.1), has larger divergence angles than the Shibantan *C. gracilis* specimens (Figs. 2.4–2.8, 3.1). Some *C. masoni* specimens from Newfoundland (Dunn et al., 2019, figs. 7, 8) exhibit a slender frond with parallel-sided margins, similar to the Shibantan *C. gracilis* specimens, and they possess a long connecting region, which has been interpreted as an artifact caused by twisting upon felling (Dunn et al., 2019) that may also be affected by water currents. However, the divergence angles of these Newfoundland specimens are larger than 20°, and their first-order branches are sigmoidal in shape (Fig. 5.5), both of which are different from *C. gracilis* specimens.

The slender, straight, and blade-like shape, and the lower divergence angle, of first-order branches of *Charnia gracilis* are therefore considered a species-level taxonomic distinction. The more or less straight first-order branches of the Shibantan *C. gracilis* specimens lead to slightly jagged lateral margins and a sharp V-shaped apex of the petalodium (Fig. 2.4). The distal end of the first-order branches of Shibantan *C. gracilis* specimens is not distinctly curved (Fig. 2.4–2.8), in contrast to *Charnia* specimens elsewhere, indicating that the lateral margins of the petalodium in *C. gracilis* may have been somewhat unfurled and not morphologically influenced by water currents when alive. A petalodium with furled lateral margins would be better streamlined to reduce the drag of water currents, whereas one with unfurled lateral margins would fully expose the surface area of the frond to water currents, thus enhancing the feeding efficiency. However, considering that both *C. gracilis* and *C. masoni* are present in the Shibantan Member, and that there are relatively few specimens of either taxon, it is difficult to distinguish whether the Shibantan specimens are furled. It is also uncertain whether furling is a persistent and taxonomically informative character, an ecophenotypic behavior related to feeding strategies and water current intensity, or a biostratinomic feature.

Previous studies proposed that the growth of *Charnia* was achieved by the insertion of new first-order branches (e.g., Laflamme et al., 2007; Antcliffe and Brasier, 2008; Laflamme and Narbonne, 2008), but recent studies hypothesized that *Charnia* grew by the insertion of new first-order branches followed by their subsequent inflation (Wilby et al., 2015; Dunn et al., 2018). Two small frondose fossils (Fig. 3.4, 3.5) from the Shibantan limestone are recognized as juvenile specimens of *C. gracilis*. Although poorly preserved, it seems that these juvenile specimens contain fewer first-order branches (~12; Fig. 3.4, 3.5) than the largest specimen in our collection (>26; Fig. 3.1), supporting insertion of new first-order branches as a key growth mechanism. However, the number of second-order branches (~12–20) in each first-order branch does not seem to change much among specimens of different sizes (Fig. 4.1), whereas the shape of the second-order branches varies from near rectangular in the small- and medium-sized specimens (e.g., Fig. 2.3, 2.4), to axially rhomboidal in large-sized specimens (e.g., Fig. 3.1, 3.2); their size also increases greatly (Fig. 4.2). Considering that first-order branches increase in number and size during growth (Fig. 5.6, 5.7) whereas second-order branches increase mainly in size rather than number in every first-order branch (Fig. 4), it seems that the inflation of first-order branches was achieved mainly by inflation of second-order branches rather than insertion of new second-order branches. These observations support the hypothesis that growth of *Charnia* was accomplished by the insertion and subsequent inflation of first-order branches (Laflamme et al., 2007; Laflamme and Narbonne, 2008; Wilby et al., 2015; Dunn et al., 2018), which grew largely by inflation rather than insertion of second-order branches. Each first-order branch is basally initiated from the third to sixth second-order branches of the subtending first-order branch in the Shibantan specimens (e.g., Fig. 2.3), similar to those described by Dunn et al. (2021). The smaller first-order branches at the apical end of the petalodium (e.g., Fig. 3.4) suggest that new first-order branches were generated distally, in contrast to the long-considered analogs of sea pens (Antcliffe and Brasier, 2007). The presence of a stem in the larger *C. masoni* specimen (Fig. 2.1) and the absence of a stem in the juvenile specimens of *C. gracilis* implies that the stem may have been absent in younger stages but emerged later in the adult stage of the *Charnia* frond. Therefore, there may have been another generative zone at the proximal end of the *Charnia* frond where the stem was generated, in addition to the apical growth zone where new first-order branches were inserted (Dunn et al., 2018).

Although *Charnia* is widely considered to have been an epibenthic organism, its posture on the seafloor has been debated. Some researchers consider it a reclining organism on the basis of the inference that most *Charnia* specimens preserve only one side of the frond, assuming that the two sides might be different (Grazhdankin, 2004; McIlroy et al., 2021). However, the twisted stem in a Shibantan *C. masoni* specimen (Fig. 2.1) implies the influence of water currents that rotated a standing frond, consistent with an erect living lifestyle (Laflamme

https://doi.org/10.1017/jpa.2022.97 Published online by Cambridge University Press

et al., 2007; Narbonne et al., 2014; Wilby et al., 2015; Droser et al., 2017). The presence of a holdfast in some *Charnia* specimens (Fig. 2.1, 2.7) is also consistent with an erect lifestyle, although holdfasts are rarely preserved or observed. Some *Charnia* specimens from other localities preserve a small and bulbous holdfast (Laflamme et al., 2007; Wilby et al., 2015; Dunn et al., 2019), which has been taken as evidence that the holdfast was buried below the sediment–water interface (Burzynski and Narbonne, 2015). One Shibantan *C. gracilis* specimen preserves a faint holdfast (Fig. 2.7), and another *C. masoni* specimen bears a distinctly larger holdfast with filiform texture (Fig. 2.1, 2.2; Table 1). It is possible that the larger holdfast illustrated in Figure 2.1 represents an uprooted specimen that was pulled out of the sediment by water currents; this interpretation is also consistent with the twisted stem in this specimen, which may have been caused by rotation of the frond relative to the holdfast because of water currents. Overall, the evidence available seems to suggest that *Charnia* stood rather than lay on the seafloor.

The occurrence of *Charnia* in the Shibantan biota expands the paleogeographic distribution of this taxon and represents one of the youngest examples of this genus. The Shibantan Member preserves taxa that were thought to be characteristic of the Nama assemblage (e.g., *Cloudina*; S. Xiao et al., 2020) and White Sea assemblage (e.g., *Dickinsonia*; Wang et al., 2021). Previous researchers regarded the Shibantan biota as an example of the Nama assemblage (Boag et al., 2016; Muscente et al., 2019; Wu et al., 2021), an example of the White Sea assemblage (Laflamme et al., 2018), or a transition between these two assemblages (S. Xiao et al., 2020). Regardless, a recent radiometric date of 543.4 ± 3.5 Ma from the overlying Baimatuo Member (Huang et al., 2020) indicates that the Shibantan biota preserves one of the youngest occurrences of *Charnia*, roughly comparable in age to two other terminal Ediacaran occurrences, in the Khatyspyt Formation in Siberia (~553–544 Ma; Grazhdankin et al., 2008; Rogov et al., 2015) and in the Zhoujieshan Formation in Qaidam (~550–539 Ma; Pang et al., 2021). Meanwhile, the oldest occurrences of *Charnia* come from the Drook Formation in Newfoundland, Canada (~574–560 Ma; Narbonne and Gehling, 2003; Matthews et al., 2021) and the Bradgate Formation in Charnwood Forest, UK (~562–557 Ma; Ford, 1958; Noble et al., 2015); the genus is also present in the White Sea assemblage (Martin et al., 2000; Gehling and Droser, 2013). In terms of paleogeographic distribution, *Charnia* has been reported from almost all major Ediacara-type fossil localities ranging from low to high paleolatitudes (Fig. 6; see also Boddy et al., 2022). In terms of paleoenvironmental distribution, *Charnia* specimens have been reported from siliciclastic sediments in deep marine basins (Hofmann et al., 2008; Liu et al., 2015) to sandstones in shallow shelf environments, including lagoon/delta front and lower shoreface (or sheet-flow sands) (Gehling and Droser, 2013; McMahon et al., 2020) to carbonate shelves (Grazhdankin et al., 2008; this paper). Thus, *Charnia* is an Ediacara-type macrofossil genus with a remarkably long stratigraphic range and broad paleogeographic range (Fig. 6). This implies that the sessile *Charnia* must have had some sort of dispersal strategies, presumably through planktonic larvae (Darroch et al., 2013) or waterborne asexual propagules (Mitchell et al., 2015; Mitchell and Kenchington, 2018; see also Liu and Dunn, 2020). In addition, a juvenile specimen of *Charnia* is preserved together with a *Helminthoidichnites*-like trace fossil (Fig. 3.3), indicating that *Charnia* could survive in an environment occupied by bilaterian trace makers. The co-occurrence of *Helminthoidichnites*-like trace fossils and Ediacara-type body

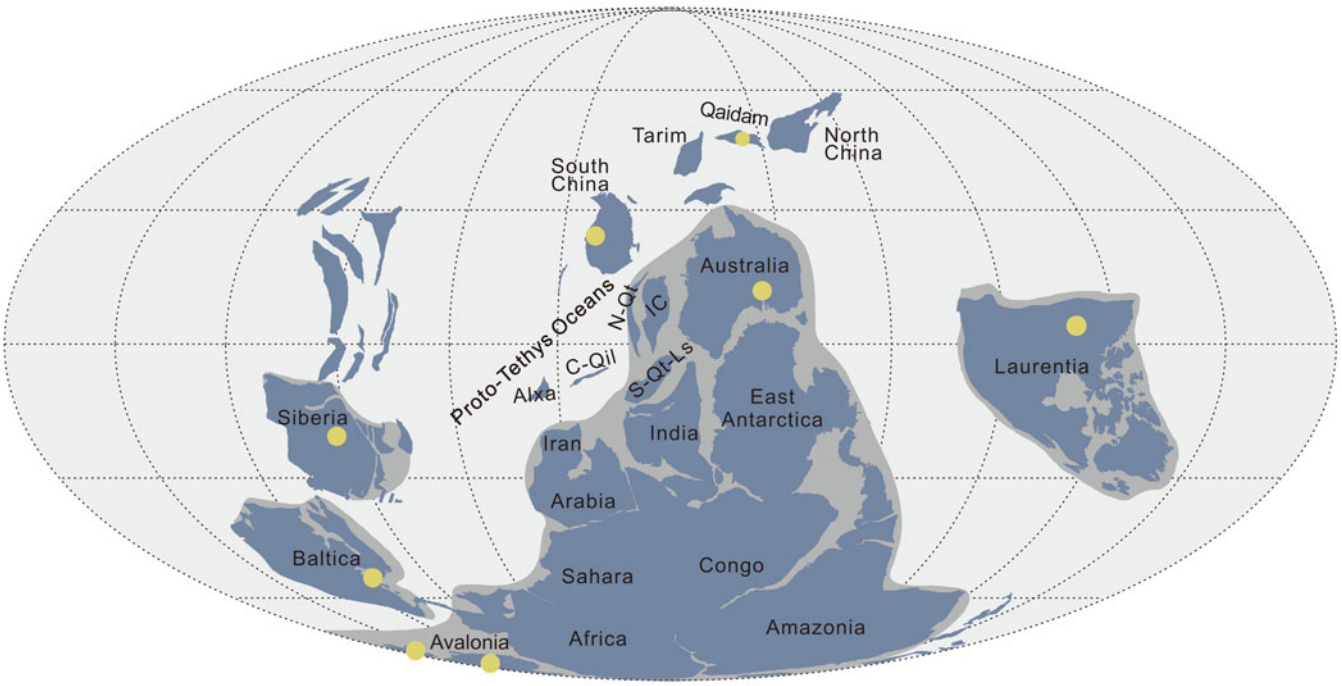

Figure 6. Paleogeographic distribution of *Charnia* (marked by yellow dots) worldwide. The paleogeographic map (~550 Ma) is based on Zhao et al. (2018) and Pang et al. (2021). C-Qil = Central Qilian; N-Qt = North Qiangtang; S-Qt-Ls = South Qiangtang and Lhasa; IC = Indochina.

https://doi.org/10.1017/jpa.2022.97 Published online by Cambridge University Press

fossils has also been observed in other Ediacaran successions (e.g., Gehling and Droser, 2018). Such co-occurrences can provide key insights into the ecological interactions between trace-making animals and Ediacara-type soft-bodied macro-organisms and may help to test the biotic replacement hypothesis that bilaterian bioturbation may have led to the demise of sessile frondose taxa in the terminal Ediacaran (e.g., Seilacher, 1989, 1992; Laflamme et al., 2013; Darroch et al., 2015).

Conclusion

A systematic description of *Charnia masoni* and *Charnia gracilis* n. sp. from the Shibantan biota (ca. 550–543 Ma) is presented in this paper. The Shibantan *C. gracilis* specimens show differences in the overall morphology, length/width ratio, and divergence angle of first-order branches from the type species, *C. masoni*. Nevertheless, morphological aspects of their first and second-order branches, their tightly constrained and one-sided first-order branches, and their zig-zag central suture indicate that they belong to the genus *Charnia*. The Shibantan *Charnia* specimens also present features that seem to support an insertion–inflation growth model and an erect sessile epibenthic lifestyle. *Charnia masoni* and *C. gracilis* from the Shibantan limestone represent one of the youngest occurrences of the genus *Charnia* and extend the paleogeographic, paleoenvironmental, and stratigraphic distributions of this genus. *Charnia* seems to be an evolutionarily resilient genus that persisted for ~30 Myr and witnessed the rise and fall of the Ediacara-type macro-organisms.

Acknowledgments

This work was supported by the National Natural Science Foundation of China (grants 42130207, 42272005, and 41921002), the Chinese Academy of Sciences (CAS) (grants XDB26000000 and QYZDJ-SSW-DQC009), the National Key Research and Development Program of China (grant 2022YFF0802700), the Youth Innovation Promotion Association of the CAS (grant 2021307), and the State Key Laboratory of Palaeobiology and Stratigraphy (20201102). We thank Associate Editor J. Schiffbauer, G. Narbonne, A. Liu, and M. Laflamme for constructive reviews.

Declaration of competing interests

The authors declare none.

References

An, Z., Jiang, G., Tong, J., Tian, L., Ye, Q., Song, H., and Song, H., 2015, Stratigraphic position of the Ediacaran Miaohe biota and its constraints on the age of the upper Doushantuo $\delta^{13}C$ anomaly in the Yangtze Gorges area, South China: Precambrian Research, v. 271, p. 243–253.

Antcliffe, J.B., and Brasier, M.D., 2007, *Charnia* and sea pens are poles apart: Journal of the Geological Society, v. 164, p. 49–51.

Antcliffe, J.B., and Brasier, M.D., 2008, *Charnia* at 50: developmental models for Ediacaran fronds: Palaeontology, v. 51, p. 11–26.

Antcliffe, J.B., Liu, A.G., Menon, L.R., McIlroy, D., McLoughlin, N., and Wacey, D., 2017, Understanding ancient life: how Martin Brasier changed the way we think about the fossil record: Geological Society, London, Special Publications, v. 448, p. 19–31.

Bamforth, E.L., and Narbonne, G.M., 2009, New Ediacaran rangeomorphs from Mistaken Point, Newfoundland, Canada: Journal of Paleontology, v. 83, p. 897–913.

Boag, T.H., Darroch, S.A.F., and Laflamme, M., 2016, Ediacaran distributions in space and time: testing assemblage concepts of earliest macroscopic body fossils: Paleobiology, v. 42, p. 574–594.

Bobrovskiy, I., Hope, J.M., Ivantsov, A., Nettersheim, B.J., Hallmann, C., and Brocks, J.J., 2018, Ancient steroids establish the Ediacaran fossil *Dickinsonia* as one of the earliest animals: Science, v. 361, p. 1246–1249.

Boddy, C.E., Mitchell, E.G., Merdith, A., and Liu, A.G., 2022, Palaeolatitudinal distribution of the Ediacaran macrobiota: Journal of the Geological Society (London), v. 179, n. jgs2021-030, https://doi.org/10.1144/jgs2021-030

Boynton, H.E., and Ford, T.D., 1995, Ediacaran fossils from the Precambrian (Charnian Supergroup) of Charnwood Forest, Leicestershire, England: Mercian Geologist, v. 13, p. 165–182.

Brasier, M.D., Antcliffe, J.B., and Liu, A.G., 2012, The architecture of Ediacaran fronds: Palaeontology, v. 55, p. 1105–1124.

Budd, G.E., and Jensen, S., 2017, The origin of the animals and a 'Savannah' hypothesis for early bilaterian evolution: Biological Reviews, v. 92, p. 446–473.

Burzynski, G., and Narbonne, G.M., 2015, The discs of Avalon: relating discoid fossils to frondose organisms in the Ediacaran of Newfoundland, Canada: Palaeogeography, Palaeoclimatology, Palaeoecology, v. 434, p. 34–45.

Butterfield, N., 2022, Constructional and functional anatomy of Ediacaran rangeomorphs: Geological Magazine, v. 159, p. 1148–1159.

Callow, R.H.T., and Brasier, M.D., 2009, Remarkable preservation of microbial mats in Neoproterozoic siliciclastic settings: implications for Ediacaran taphonomic models: Earth-Science Reviews, v. 96, p. 207–219.

Chen, X., Zhou, P., Zhang, B., Wei, K., and Zhang, M., 2016, Lithostratigraphy, biostratigraphy, sequence stratigraphy and carbon isotope chemostratigraphy of the upper Ediacaran in Yangtze Gorges and their significance for chronostratigraphy: Geology and Mineral Resources of South China, v. 32, p. 87–105.

Chen, Z., Zhou, C., Meyer, M., Xiang, K., Schiffbauer, J.D., Yuan, X., and Xiao, S., 2013, Trace fossil evidence for Ediacaran bilaterian animals with complex behaviors: Precambrian Research, v. 224, p. 690–701.

Chen, Z., Zhou, C., Xiao, S., Wang, W., Guan, C., Hua, H., and Yuan, X., 2014, New Ediacara fossils preserved in marine limestone and their ecological implications: Scientific Reports, v. 4, n. 4180, https://doi.org/10.1038/srep04180

Chen, Z., Zhou, C., Yuan, X., and Xiao, S., 2019, Death march of a segmented and trilobate bilaterian elucidates early animal evolution: Nature, v. 573, p. 412–415.

Condon, D., Zhu, M., Bowring, S., Wang, W., Yang, A., and Jin, Y., 2005, U–Pb ages from the Neoproterozoic Doushantuo Formation, China: Science, v. 308, p. 95–98.

Darroch, S.A.F., Laflamme, M., and Clapham, M.E., 2013, Population structure of the oldest known macroscopic communities from Mistaken Point, Newfoundland: Paleobiology, v. 39, p. 591–608.

Darroch, S.A.F. et al., 2015, Biotic replacement and mass extinction of the Ediacara biota: Proceedings of the Royal Society of London B: Biological Sciences, v. 282, n. 20151003, https://doi.org/10.1098/rspb.2015.1003

Darroch, S.A.F., Smith, E.F., Laflamme, M., and Erwin, D.H., 2018, Ediacaran extinction and Cambrian Explosion: Trends in Ecology & Evolution, v. 33, p. 653–663.

Dececchi, T.A., Narbonne, G.M., Greentree, C., and Laflamme, M., 2017, Relating Ediacaran fronds: Paleobiology, v. 43, p. 171–180.

Dececchi, T.A., Narbonne, G.M., Greentree, C., and Laflamme, M., 2018, Phylogenetic relationships among the Rangeomorpha: the importance of outgroup selection and implications for their diversification: Canadian Journal of Earth Sciences, v. 55, p. 1223–1239.

Ding, W., Dong, L., Sun, Y., Ma, H., Xu, Y., Yang, R., Peng, Y., Zhou, C., and Shen, B., 2019, Early animal evolution and highly oxygenated seafloor niches hosted by microbial mats: Scientific Reports, v. 9, n. 13628, https://doi.org/10.1038/s41598-019-49993-2

Ding, Y., Chen, D., Zhou, X., Guo, C., Huang, T., and Zhang, G., 2019, Cavity-filling dolomite speleothems and submarine cements in the Ediacaran Dengying microbialites, South China: responses to high-frequency sea-level fluctuations in an 'aragonite–dolomite sea': Sedimentology, v. 66, p. 2511–2537.

Droser, M.L., Tarhan, L.G., and Gehling, J.G., 2017, The rise of animals in a changing environment: global ecological innovation in the late Ediacaran: Annual Review of Earth and Planetary Sciences, v. 45, p. 593–617.

Duda, J.-P., Zhu, M., and Reitner, J., 2016, Depositional dynamics of a bituminous carbonate facies in a tectonically induced intra-platform basin: the Shibantan Member (Dengying Formation, Ediacaran Period): Carbonates and Evaporites, v. 31, p. 87–99.

Dufour, S.C., and McIlroy, D., 2016, Ediacaran pre-placozoan diploblasts in the Avalonian biota: the role of chemosynthesis in the evolution of early

https://doi.org/10.1017/jpa.2022.97 Published online by Cambridge University Press

animal life: Geological Society, London, Special Publications, v. 448, p. 211–219.
Dunn, F.S., Liu, A.G., and Donoghue, P.C.J., 2018, Ediacaran developmental biology: Biological Reviews, v. 93, p. 914–932.
Dunn, F.S., Wilby, P.R., Kenchington, C.G., Grazhdankin, D.V., Donoghue, P.C., and Liu, A.G., 2019, Anatomy of the Ediacaran rangeomorph *Charnia masoni*: Papers in Palaeontology, v. 5, p. 157–176.
Dunn, F.S., Liu, A.G., Grazhdankin, D.V., Vixseboxse, P., Flannery-Sutherland, J., Green, E., Harris, S., Wilby, P.R., and Donoghue, P.C.J., 2021, The developmental biology of *Charnia* and the eumetazoan affinity of the Ediacaran rangeomorphs: Science Advances, v. 7, n. eabe0291, https://doi.org/10.1126/sciadv.abe0291
Fedonkin, M.A., 1978, New locality of nonskeletal Metazoa in Vendian of Winter Shore: Doklady Akademii Nauk SSSR, v. 239, p. 1423–1426.
Fedonkin, M.A., 1981a, White Sea biota of the Vendian: Trudy Geologicheskiy Institut, v. 342, p. 1–100.
Fedonkin, M.A., 1981b, A major locality of Precambrian: Priroda, v. 5, p. 94–102.
Fedonkin, M.A., 1983a, Ecology of Precambrian Metazoa of the White Sea biota, *in* Problems of Ecology of Fauna and Flora in Ancient Basins: Proceedings of the Paleontological Institute of the Academy of Sciences of the USSR, v. 194: Moscow, Nauka, p. 25–33.
Fedonkin, M.A., 1983b, Organic world of the Vendian: Itogi Nauki i Tekhniki, seriya Stratigrafiya, Paleontologiya, v. 12, p. 1–127.
Fedonkin, M.A., 1985, Systematic description of Vendian Metazoa, *in* Sokolov, B.S., and Iwanowski, A.B., eds., The Vendian System. Volume 1. Paleontology: Moscow, Nauka, p. 70–112.
Fedonkin, M.A., 1987, Non-skeletal fauna of the Vendian and its place in the evolution of metazoans: Trudy Paleontologicheskogo Instituta Akademii Nauk SSSR, v. 226, p. 1–173.
Fedonkin, M.A., 1990, Systematic description of Vendian Metazoa, *in* Sokolov, B S., and Iwanowski, A.B., eds., The Vendian System. Volume 1. Paleontology: Heidelberg, Springer-Verlag, p. 71–120.
Fedonkin, M.A., 1992, Vendian faunas and the early evolution of Metazoa, *in* Lipps, J., and Signor, P., eds., Origin and Early Evolution of the Metazoa, v. 10: Boston, Springer, p. 87–129.
Fedonkin, M.A., 1994, Vendian body fossils and trace fossils, *in* Bengtson, S., ed., Early Life on Earth: New York, Columbia University Press, p. 370–388.
Fedonkin, M.A., and Waggoner, B.M., 1997, The Late Precambrian fossil *Kimberella* is a mollusc-like bilaterian organism: Nature, v. 388, p. 868–871.
Fedonkin, M.A., Gehling, J.G., Grey, K., Narbonne, G.M., and Vickers-Rich, P., 2007, The Rise of Animals: Evolution and Diversification of the Kingdom Animalia: Baltimore, Johns Hopkins University Press, 326 p.
Ford, T.D., 1958, Pre-Cambrian fossils from Charnwood Forest: Proceedings of the Yorkshire Geological Society, v. 31, p. 211–217.
Ford, T.D., 1962, The oldest fossils: New Scientist, v. 15, p. 191–194.
Ford, T.D., 1999, The Precambrian fossils of Charnwood Forest: Geology Today, v. 15, p. 230–234.
Gehling, J.G., 1991, The case for Ediacaran fossil roots to the metazoan tree: Geological Society of India Memoir, v. 20, p. 181–224.
Gehling, J.G., 1999, Microbial mats in terminal Proterozoic siliciclastics: Ediacaran death masks: Palaios, v. 14, p. 40–57.
Gehling, J.G., and Droser, M.L., 2013, How well do fossil assemblages of the Ediacara Biota tell time?: Geology, v. 41, p. 447–450.
Gehling, J.G., and Droser, M.L., 2018, Ediacaran scavenging as a prelude to predation: Emerging Topics in Life Sciences, v. 2, p. 213–222.
Germs, G.J.B., 1973, A reinterpretation of *Rangea schneiderhoehni* and the discovery of a related new fossil from the Nama Group, South West Africa: Lethaia, v. 6, p. 1–9.
Ghisalberti, M., Gold, D.A., Laflamme, M., Clapham, M.E., Narbonne, G.M., Summons, R.E., Johnston, D.T., and Jacobs, D.K., 2014, Canopy flow analysis reveals the advantage of size in the oldest communities of multicellular eukaryotes: Current Biology, v. 24, p. 305–309.
Glaessner, M.F., 1959, Precambrian Coelenterata from Australia, Africa and England: Nature, v. 183, p. 1472–1473.
Glaessner, M.F., 1961, Pre-Cambrian animals: Scientific American, v. 204, p. 72–78.
Glaessner, M.F., 1962, Pre-Cambrian fossils: Biological Reviews, v. 37, p. 467–493.
Glaessner, M.F., 1979, Precambrian, *in* Moore, R.C., Robinson, R.A., and Teichert, C., eds., Treatise on Invertebrate Paleontology, Part A, Fossilization (Taphonomy), Biogeography and Biostratigraphy, Introduction: Boulder, Colorado, and Lawrence, Kansas, Geological Society of America and University of Kansas Press, p. 79–118.
Glaessner, M.F., 1984, The Dawn of Animal Life: A Biohistorical Study: Cambridge, Cambridge University Press, 244 p.
Glaessner, M.F., and Daily, B., 1959, The geology and late Precambrian fauna of the Ediacara fossil reserve: Records of the South Australian Museum, v. 13, p. 369–401.
Glaessner, M.F., and Wade, M., 1966, The late Precambrian fossils from Ediacara, South Australia: Palaeontology, v. 9, p. 599–628.
Glaessner, M.F., and Walter, M.R., 1981, Australian Precambrian palaeobiology: Developments in Precambrian Geology, v. 2, p. 361–396.
Grazhdankin, D.V., 2004, Patterns of distribution in the Ediacaran biotas: facies versus biogeography and evolution: Paleobiology, v. 30, p. 203–221.
Grazhdankin, D., 2011, Ediacaran Biota, *in* Reitner, J., and Thiel, V., eds., Encyclopedia of Geobiology: Dordrecht, Springer, p. 342–348.
Grazhdankin, D., 2014, Patterns of evolution of the Ediacaran soft-bodied biota: Journal of Paleontology, v. 88, p. 269–283.
Grazhdankin, D., and Bronnikov, A., 1997, A new locality of the remains of the late Vendian soft-bodied organisms on the Onega Peninsula: Transactions (Doklady) of the Russian Academy of Sciences/Earth Science Sections, v. 357A, p. 1311–1315.
Grazhdankin, D., Maslov, A., Mustill, T., and Krupenin, M., 2005, The Ediacaran White Sea biota in the Central Urals: Doklady Earth Sciences, v. 401, p. 382–385.
Grazhdankin, D.V., Balthasar, U., Nagovitsin, K.E., and Kochnev, B.B., 2008, Carbonate-hosted Avalon-type fossils in arctic Siberia: Geology, v. 36, p. 803–806.
Hofmann, H.J., O'Brien, S.J., and King, A.F., 2008, Ediacaran biota on Bonavista Peninsula, Newfoundland, Canada: Journal of Paleontology, v. 82, p. 1–36.
Hoyal Cuthill, J.F., and Han, J., 2018, Cambrian petalonamid *Stromatoveris* phylogenetically links Ediacaran biota to later animals: Palaeontology, v. 61, p. 813–823.
Huang, T., Chen, D., Ding, Y., Zhou, X., and Zhang, G., 2020, SIMS U–Pb zircon geochronological and carbon isotope chemostratigraphic constraints on the Ediacaran–Cambrian boundary succession in the Three Gorges Area, South China: Journal of Earth Science, v. 31, p. 69–78.
Jenkins, R.J.F., 1985, The enigmatic Ediacaran (late Precambrian) genus *Rangea* and related forms: Paleobiology, v. 11, p. 336–355.
Jenkins, R.J.F., 1996, Aspects of the geological setting and palaeobiology of the Ediacara assemblage, *in* Davies, M., Twidale, C.R., and Tyler, M.J., eds., Natural History of the Flinders Ranges, v. 7: Richmond, South Australia, Royal Society of South Australia, p. 33–45.
Kenchington, C.G., Harris, S.J., Vixseboxse, P.B., Pickup, C., and Wilby, P.R., 2018, The Ediacaran fossils of Charnwood Forest: shining new light on a major biological revolution: Proceedings of the Geologists' Association, v. 129, p. 264–277.
Laflamme, M., and Narbonne, G.M., 2008, Ediacaran fronds: Palaeogeography, Palaeoclimatology, Palaeoecology, v. 258, p. 162–179.
Laflamme, M., Narbonne, G.M., Greentree, C., and Anderson, M.M., 2007, Morphology and taphonomy of an Ediacaran frond: *Charnia* from the Avalon Peninsula of Newfoundland, *in* Vickers-Rich, P., and Komarower, P., eds., The Rise and Fall of the Ediacaran Biota: London, Geological Society, p. 237–257.
Laflamme, M., Xiao, S., and Kowalewski, M., 2009, Osmotrophy in modular Ediacara organisms: Proceedings of the National Academy of Sciences, v. 106, p. 14438–14443.
Laflamme, M., Schiffbauer, J.D., Narbonne, G.M., and Briggs, D.E.G., 2011, Microbial biofilms and the preservation of the Ediacara biota: Lethaia, v. 44, p. 203–213.
Laflamme, M., Darroch, S.A.F., Tweedt, S.M., Peterson, K.J., and Erwin, D.H., 2013, The end of the Ediacara biota: extinction, biotic replacement, or Cheshire Cat?: Gondwana Research, v. 23, p. 558–573.
Laflamme, M., Gehling, J.G., and Droser, M.L., 2018, Deconstructing an Ediacaran frond: three-dimensional preservation of *Arborea* from Ediacara, South Australia: Journal of Paleontology, v. 92, p. 323–335.
Liang, D., Cai, Y., Nolan, M., and Xiao, S., 2020, The terminal Ediacaran tubular fossil *Cloudina* in the Yangtze Gorges area of South China: Precambrian Research, v. 351, n. 105931, https://doi.org/10.1016/j.precamres.2020.105931
Linnemann, U. et al., 2019, New high-resolution age data from the Ediacaran–Cambrian boundary indicate rapid, ecologically driven onset of the Cambrian explosion: Terra Nova, v. 31, p. 49–58.
Liu, A.G., and Dunn, F.S., 2020, Filamentous connections between Ediacaran fronds: Current Biology, v. 30, p. 1322–1328.
Liu, A.G., McIlroy, D., Matthews, J.J., and Brasier, M.D., 2012, A new assemblage of juvenile Ediacaran fronds from the Drook Formation, Newfoundland: Journal of the Geological Society, v. 169, p. 395–403.
Liu, A.G., McIlroy, D., Matthews, J.J., and Brasier, M.D., 2013, Exploring an Ediacaran 'nursery': growth, ecology and evolution in a rangeomorph palaeocommunity: Geology Today, v. 29, p. 23–26.
Liu, A.G., Kenchington, C.G., and Mitchell, E.G., 2015, Remarkable insights into the paleoecology of the Avalonian Ediacaran macrobiota: Gondwana Research, v. 27, p. 1355–1380.
Liu, A.G., Matthews, J.J., and McIlroy, D., 2016, The *Beothukis*/*Culmofrons* problem and its bearing on Ediacaran macrofossil taxonomy: evidence from an exceptional new fossil locality: Palaeontology, v. 59, p. 45–58.

https://doi.org/10.1017/jpa.2022.97 Published online by Cambridge University Press

Luzhnaya, E., and Ivantsov, A.Y., 2019, Skeletal nets of the Ediacaran fronds: Paleontological Journal, v. 53, p. 667–675.
Martin, M.W., Grazhdankin, D.V., Bowring, S.A., Evans, D.A.D., Fedonkin, M.A., and Kirschvink, J.L., 2000, Age of Neoproterozoic bilatarian body and trace fossils, White Sea, Russia: implications for metazoan evolution: Science, v. 288, p. 841–845.
Matthews, J.J., Liu, A.G., Yang, C., McIlroy, D., Levell, B., and Condon, D.J., 2021, A chronostratigraphic framework for the rise of the Ediacaran macrobiota: new constraints from Mistaken Point Ecological Reserve, Newfoundland: GSA Bulletin, v. 133, p. 612–624.
McIlroy, D., Dufour, S.C., Taylor, R., and Nicholls, R., 2021, The role of symbiosis in the first colonization of the seafloor by macrobiota: insights from the oldest Ediacaran biota (Newfoundland, Canada): BioSystems, v. 205, n. 104413, https://doi.org/10.1016/j.biosystems.2021.104413
McIlroy, D., Hawco, J., McKean, C., Nicholls, R., Pasinetti, G., and Taylor, R., 2022, Palaeobiology of the reclining rangeomorph *Beothukis* from the Ediacaran Mistaken Point Formation of southeastern Newfoundland: Geological Magazine, v. 159, p. 1160–1174.
McMahon, W.J., Liu, A.G., Tindal, B.H., and Kleinhans, M.G., 2020, Ediacaran life close to land: coastal and shoreface habitats of the Ediacaran macrobiota, the Central Flinders Ranges, South Australia: Journal of Sedimentary Research, v. 90, p. 1463–1499.
Meyer, M., Xiao, S., Gill, B.C., Schiffbauer, J.D., Chen, Z., Zhou, C., and Yuan, X., 2014, Interactions between Ediacaran animals and microbial mats: insights from *Lamonte trevallis*, a new trace fossil from the Dengying Formation of South China: Palaeogeography, Palaeoclimatology, Palaeoecology, v. 396, p. 62–74.
Mitchell, E.G., and Kenchington, C.G., 2018, The utility of height for the Ediacaran organisms of Mistaken Point: Nature Ecology & Evolution, v. 2, p. 1218–1222.
Mitchell, E.G., Kenchington, C.G., Liu, A.G., Matthews, J.J., and Butterfield, N.J., 2015, Reconstructing the reproductive mode of an Ediacaran macroorganism: Nature, v. 524, p. 343–346.
Moynihan, D.P., Strauss, J.V., Nelson, L.L., and Padget, C.D., 2019, Upper Windermere Supergroup and the transition from rifting to continent-margin sedimentation, Nadaleen River area, northern Canadian Cordillera: GSA Bulletin, v. 131, p. 1673–1701.
Muscente, A.D. et al., 2019, Ediacaran biozones identified with network analysis provide evidence for pulsed extinctions of early complex life: Nature Communications, v. 10, n. 911, https://doi.org/10.1038/s41467-019-08837-3
Narbonne, G.M., 2004, Modular construction of early Ediacaran complex life forms: Science, v. 305, p. 1141–1144.
Narbonne, G.M., and Gehling, J.G., 2003, Life after snowball: the oldest complex Ediacaran fossils: Geology, v. 31, p. 27–30.
Narbonne, G., Dalrymple, R., Laflamme, M., Gehling, J., and Boyce, W., 2005, Life after snowball: Mistaken Point Biota and the Cambrian of the Avalon. North American Paleontological Convention Field Trip Guidebook: Halifax, North American Paleontology Convention, 100 p.
Narbonne, G.M., Laflamme, M., Greentree, C., and Trusler, P., 2009, Reconstructing a lost world: Ediacaran rangeomorphs from Spaniard's Bay, Newfoundland: Journal of Paleontology, v. 83, p. 503–523.
Narbonne, G.M., Laflamme, M., Trusler, P.W., Dalrymple, R.W., and Greentree, C., 2014, Deep-water Ediacaran fossils from northwestern Canada: taphonomy, ecology, and evolution: Journal of Paleontology, v. 88, p. 207–223.
Nedin, C., and Jenkins, R.J.F., 1998, First occurrence of the Ediacaran fossil *Charnia* from the Southern Hemisphere: Alcheringa, v. 22, p. 315–316.
Noble, S.R., Condon, D.J., Carney, J.N., Wilby, P.R., Pharaoh, T.C., and Ford, T.D., 2015, U–Pb geochronology and global context of the Charnian Supergroup, UK: constraints on the age of key Ediacaran fossil assemblages: GSA Bulletin, v. 127, p. 250–265.
Okada, Y., Sawaki, Y., Komiya, T., Hirata, T., Takahata, N., Sano, Y., Han, J., and Maruyama, S., 2014, New chronological constraints for Cryogenian to Cambrian rocks in the Three Gorges, Weng'an and Chengjiang areas, South China: Gondwana Research, v. 25, p. 1027–1044.
Pang, K., Wu, C., Sun, Y., Ouyang, Q., Yuan, X., Shen, B., Lang, X., Wang, R., Chen, Z., and Zhou, C., 2021, New Ediacara-type fossils and late Ediacaran stratigraphy from the northern Qaidam Basin (China): paleogeographic implications: Geology, v. 49, p. 1160–1164.
Peterson, K.J., Waggoner, B., and Hagadorn, J.W., 2003, A fungal analog for Newfoundland Ediacaran fossils?: Integrative and Comparative Biology, v. 43, p. 127–136.
Pflug, H.D., 1970, Zur Fauna der Nama-Schichten in Südwest-Afrika. II. Rangeidae, Bau und Systematische Zugehörigkeit: Palaeontographica Abteilung A, v. 135, p. 198–231.
Pflug, H.D., 1972, Zur Fauna der Nama-Schichten in Südwest-Afrika. III. Erniettomorpha, Bau and Systematik: Palaeontographica Abteilung A, v. 139, p. 134–170.
Preiss, W.V., 1987, The Adelaide Geosyncline: Late Proterozoic Stratigraphy, Sedimentation, Palaeontology and Tectonics: Bulletin of the Geological Survey of South Australia, v. 53, 438 p.
Retallack, G.J., 1994, Were the Ediacaran fossils lichens?: Paleobiology, v. 20, p. 523–544.
Rogov, V.I., Karlova, G.A., Marusin, V.V., Kochnev, B.B., Nagovitsin, K.E., and Grazhdankin, D.V., 2015, Duration of the first biozone in the Siberian hypostratotype of the Vendian: Russian Geology and Geophysics, v. 56, p. 573–583.
Runnegar, B.N., 2022, Following the logic behind biological interpretations of the Ediacaran biotas: Geological Magazine, v. 159, p. 1093–1117.
Runnegar, B.N., and Fedonkin, M.A., 1992, Proterozoic metazoan body fossils, *in* Schopf, J.W., and Klein, C., eds., The Proterozoic Biosphere: A Multidisciplinary Study: Cambridge, Cambridge University Press, p. 369–388.
Seilacher, A., 1989, Vendozoa: organismic construction in the Proterozoic biosphere: Lethaia, v. 22, p. 229–239.
Seilacher, A., 1992, Vendobionta and Psammocorallia: lost constructions of Precambrian evolution: Journal of the Geological Society, v. 149, p. 607–613.
Shao, Y., Chen, Z., Zhou, C., and Yuan, X., 2019, *Hiemalora stellaris* from the Ediacaran Dengying Formation in the Yangtze Gorges area, Hubei Province: affinity and taphonomic analysis: Acta Palaeontologica Sinica, v. 58, p. 1–10.
Sokolov, B.S., 1972a, Precambrian biosphere in light of paleontological data: Vestnik Akademii Nauk SSSR, v. 8, p. 48–54.
Sokolov, B.S., 1972b, The Vendian stage in Earth history, *in* Sokolov, B.S., ed., Proceedings of the 24th Session of the International Geological Congress: Reports of Soviet Geologists: Moscow, Nauka, p. 114–124.
Sokolov, B.S., 1973, Vendian of Northern Eurasia, *in* Pitcher, M. G., ed., Arctic Geology: American Association of Petroleum Geologists, Memoir 19, p. 204–218.
Sokolov, B.S., 1976, Organic world of the Earth on its way to Phanerozoic differentiation: Vestnik Akademii Nauk SSSR, v. 1, p. 126–143.
Sokolov, B.S., 1977, Organic world of the Earth on its way to Phanerozoic differentiation, *in* The 250th Anniversary of the Academy of Sciences of the USSR. Documents and Records of the Celebrations: Moscow, Nauka, p. 423–444.
Sokolov, B.S., 1984, Vendian period in the Earth's history: Priroda, v. 12, p. 3–18.
Sokolov, B.S., and Brekhovskikh, L.M., 1981, The progress of Earth sciences: Zemlya i Vselennaya, v. 1, p. 2–7.
Sokolov, B.S., and Fedonkin, M.A., 1983, Another 100 million years: Nauka v SSSR, v. 5, p. 10–19.
Sokolov, B.S., and Fedonkin, M.A., 1984, The Vendian as the terminal system of the Precambrian: Episodes Journal of International Geoscience, v. 7, p. 12–19.
Sperling, E.A., and Vinther, J., 2010, A placozoan affinity for *Dickinsonia* and the evolution of late Proterozoic metazoan feeding modes: Evolution & Development, v. 12, p. 201–209.
Tarhan, L.G., Droser, M.L., and Gehling, J.G., 2010, Taphonomic controls on Ediacaran diversity: uncovering the holdfast origin of morphologically variable enigmatic structures: Palaios, v. 25, p. 823–830.
Vickers-Rich, P. et al., 2013, Reconstructing *Rangea*: new discoveries from the Ediacaran of Southern Namibia: Journal of Paleontology, v. 87, p. 1–15.
Waggoner, B., 2003, The Ediacaran biotas in space and time: Integrative and Comparative Biology, v. 43, p. 104–113.
Wang, X., Pang, K., Chen, Z., Wan, B., Xiao, S., Zhou, C., and Yuan, X., 2020, The Ediacaran frondose fossil *Arborea* from the Shibantan limestone of South China: Journal of Paleontology, v. 94, p. 1034–1050.
Wang, X., Chen, Z., Pang, K., Zhou, C., Xiao, S., Wan, B., and Yuan, X., 2021, *Dickinsonia* from the Ediacaran Dengying Formation in the Yangtze Gorges area, South China: Palaeoworld, v. 30, p. 602–609.
Wilby, P.R., Carney, J.N., and Howe, M.P.A., 2011, A rich Ediacaran assemblage from eastern Avalonia: evidence of early widespread diversity in the deep ocean: Geology, v. 39, p. 655–658.
Wilby, P.R., Kenchington, C.G., and Wilby, R.L., 2015, Role of low intensity environmental disturbance in structuring the earliest (Ediacaran) macrobenthic tiered communities: Palaeogeography, Palaeoclimatology, Palaeoecology, v. 434, p. 14–27.
Wu, C., Chen, Z., Pang, K., Wang, X., Wan, B., Zhou, C., and Yuan, X., 2021, The Ediacaran Shibantan biota in the Yangtze Gorges area: perspectives from quantitative paleontology and ecospace occupancy: Acta Palaeontologica Sinica, v. 60, p. 42–68.
Xiao, Q., She, Z., Wang, G., Li, Y., Ouyang, G., Cao, K., Mason, R., and Du, Y., 2020, Terminal Ediacaran carbonate tempestites in the eastern Yangtze Gorges area, South China: Palaeogeography, Palaeoclimatology, Palaeoecology, v. 547, n. 109681, https://doi.org/10.1016/j.palaeo.2020.109681
Xiao, S., and Laflamme, M., 2009, On the eve of animal radiation: phylogeny, ecology and evolution of the Ediacara biota: Trends in Ecology & Evolution, v. 24, p. 31–40.

Xiao, S., Bykova, N., Kovalick, A., and Gill, B.C., 2017, Stable carbon isotopes of sedimentary kerogens and carbonaceous macrofossils from the Ediacaran Miaohe Member in South China: implications for stratigraphic correlation and sources of sedimentary organic carbon: Precambrian Research, v. 302, p. 171–179.

Xiao, S., Chen, Z., Zhou, C., and Yuan, X., 2019, Surfing in and on microbial mats: oxygen-related behavior of a terminal Ediacaran bilaterian animal: Geology, v. 47, p. 1054–1058.

Xiao, S., Chen, Z., Pang, K., Zhou, C., and Yuan, X., 2020, The Shibantan Lagerstätte: insights into the Proterozoic–Phanerozoic transition: Journal of the Geological Society, v. 178, n. jgs2020–135, https://doi.org/10.1144/jgs2020-135

Yang, C., Rooney, A.D., Condon, D.J., Li, X., Grazhdankin, D.V., Bowyer, F.T., Hu, C., Macdonald, F.A., and Zhu, M., 2021, The tempo of Ediacaran evolution: Science Advances, v. 7, n. eabi9643, https://doi.org/10.1126/sciadv.abi9643

Zhang, L., Chang, S., Chen, C., Wang, X., Feng, Q., Steiner, M., Yang, B., Mason, R., She, Z., and Yan, J., 2022, *Cloudina* aggregates from the uppermost Dengying Formation, Three Gorges area, South China, and stratigraphical implications: Precambrian Research, v. 370, n. 106552, https://doi.org/10.1016/j.precamres.2021.106552

Zhao, G., Wang, Y., Huang, B., Dong, Y., Li, S., Zhang, G., and Yu, S., 2018, Geological reconstructions of the East Asian blocks: from the breakup of Rodinia to the assembly of Pangea: Earth-Science Reviews, v. 186, p. 262–286.

Zhou, C., Xiao, S., Wang, W., Guan, C., Ouyang, Q., and Chen, Z., 2017, The stratigraphic complexity of the middle Ediacaran carbon isotopic record in the Yangtze Gorges area, South China, and its implications for the age and chemostratigraphic significance of the Shuram excursion: Precambrian Research, v. 288, p. 23–38.

Accepted: 23 September 2022